

Research Article: New Research / Disorders of the Nervous System

Overweighed mice show coordinated homeostatic and hedonic transcriptional response across brain

I. De Toma^{1,2}, I. E. Grabowicz^{3,4}, M. Fructuoso^{1,2}, D. Trujillano^{1,2}, B. Wilczynski³ and M. Dierssen^{1,2,5}

¹Cellular & Systems Neurobiology, Systems Biology Program, Centre for Genomic Regulation (CRG), The Barcelona Institute of Science and Technology, Dr. Aiguader 88, 08003 Barcelona, Spain

²Universitat Pompeu Fabra (UPF), Barcelona, Spain

³Institute of Informatics, Faculty of Mathematics, Informatics and Mechanics, University of Warsaw, Warsaw, Poland

⁴Postgraduate School of Molecular Medicine, Medical University of Warsaw, Warsaw, Poland

⁵Centro de Investigación Biomédica en Red de Enfermedades Raras (CIBERER), Spain

<https://doi.org/10.1523/ENEURO.0287-18.2018>

Received: 24 July 2018

Revised: 9 October 2018

Accepted: 15 October 2018

Published: 26 November 2018

Author Contributions: MD and BW conceived the project. IDT wrote most of the manuscript and performed most of the bioinformatics analysis. IG wrote the part concerning the Kruskal-Wallis test, and developed the code for TAD visualization. MD took care of the behavioral experiment and DT of the microarray experiment. MF did the statistics of the feeding behavior and wrote the behavioral part of the manuscript. MD and BW supervised and revised the work, planned the experiments, revised the results and manuscript and coordinated the project.

Funding: Ministry of economy and Competitiveness (Spain)
Severo Ochoa 2013-2017'
SAF2013-49129-C2-1-R and SAF2016-79956-R

Funding: Marie Curie IMPULSE

Funding: <http://doi.org/10.13039/501100001872>Centre for Industrial Technological Development (CDTI)
Smartfoods

Funding: Era-net-Neuron
PCIN-2013- 060

Funding: Polish National Center for Research and Development
Era-net-Neuron/10/2013

Conflict of Interest: Authors report no conflict of interest.

The authors wish it to be known that, in their opinion, the first 2 authors should be regarded as joint First Authors.

Correspondence should be addressed to Bartek Wilczynski Tel: +48 22 5544 577; Email: bartek@mimuw.edu.pl; Banacha 2, 02-097 Warszawa, Polonia; Mara Dierssen: Tel: +34-93-3160140; Fax: +34-93-3160099; Email: mara.dierssen@crg.eu; Carrer del Dr. Aiguader, 88, 08003 Barcelona

Cite as: eNeuro 2018; 10.1523/ENEURO.0287-18.2018

Alerts: Sign up at <https://www.pew-research.org/alerts> to receive customized email alerts when the full formatted version of this article is published.

1. Overweighed mice show coordinated homeostatic and hedonic transcriptional response across brain

2. Coordinated transcription in overweighed mice brain

3. List all Author Names and Affiliations in order as they would appear in the published article

De Toma I^{1,2}, Grabowicz IE^{3,4}, Fructuoso M^{1,2}, Trujillano D^{1,2}, Wilczynski B^{3,*}, Dierssen M^{1,2,5,*}

¹Cellular & Systems Neurobiology, Systems Biology Program, Centre for Genomic Regulation (CRG), The Barcelona Institute of Science and Technology, Dr. Aiguader 88, 08003 Barcelona, Spain

²Universitat Pompeu Fabra (UPF), Barcelona, Spain

³Institute of Informatics, Faculty of Mathematics, Informatics and Mechanics, University of Warsaw, Warsaw, Poland

⁴Postgraduate School of Molecular Medicine, Medical University of Warsaw, Warsaw, Poland

⁵Centro de Investigación Biomédica en Red de Enfermedades Raras (CIBERER), Spain

The authors wish it to be known that, in their opinion, the first 2 authors should be regarded as joint First Authors.

4. Author Contributions: MD and BW conceived the project. IDT wrote most of the manuscript and performed most of the bioinformatics analysis. IG wrote the part concerning the Kruskal-Wallis test, and developed the code for TAD visualization. MD took care of the behavioral experiment and DT of the microarray experiment. MF did the statistics of the feeding behavior and wrote the behavioral part of the manuscript. MD and BW supervised and revised the work, planned the experiments, revised the results and manuscript and coordinated the project.

5. Correspondence should be addressed to (include email address)

Bartek Wilczyński Tel: +48 22 5544 577; Email: bartek@mimuw.edu.pl; Banacha 2, 02-097 Warszawa, Polonia

Mara Dierssen: Tel: +34-93-3160140; Fax: +34-93-3160099; Email: mara.dierssen@crg.eu; Carrer del Dr. Aiguader, 88, 08003 Barcelona

6. Number of Figures: 5

7. Number of Tables: 8

8. Number of

Multimedia: 1

9. Number of words for Abstract: 153

10. Number of words for Significance Statement: 113

11. Number of words for Introduction: 406

12. Number of words for Discussion: 1699

13. Acknowledgements and 15. Funding sources

We are grateful to the work of Jerome McDonald in the behavioural experiments. This work was supported by the Spanish Ministry of Economy and Competitiveness; 'Centro de Excelencia Severo Ochoa 2013-2017'; the 'Centres de Recerca de Catalunya' Programme / Generalitat de Catalunya'; the Centro de Investigación Biomédica en Red Enfermedades Raras (CIBER) of Rare Diseases; DIUE de la Generalitat de Catalunya [Grups consolidats SGR 2014/1125]; Ministerio de Economía, Industria y Competitividad de España MINECO [SAF2013-49129-C2-1-R and SAF2016-79956-R]; Centro para el Desarrollo Tecnológico Industrial CDTI ["Smartfoods"]; IMPULSE (to I.D.T); the Marie-Curie program; European Union [Era Net Neuron PCIN-2013- 060] and the Polish National Center for Research and Development grant [ERA-NET-NEURON/10/2013 to B.W. and I.E.G.]. New affiliation for IG: Institute of Computer Science Polish Academy of Sciences

14. Conflict of Interest: Authors report no conflict of interest

Abstract

Obesogenic diets lead to overeating and obesity by inducing the expression of genes involved in hedonic and homeostatic responses in specific brain regions. However, how the effects on gene expression are coordinated in the brain so far remains largely unknown. In our study, we provided mice with access to energy-dense diet, which induced overeating and overweight, and we explored the transcriptome changes across the main regions involved in feeding and energy balance: hypothalamus, frontal cortex and striatum. Interestingly, we detected two regulatory processes: a switch-like regulation with differentially expressed genes changing over 1.5-fold, and "fine-tuned" subtler changes of genes whose levels correlated with body weight and behavioral changes. We found that genes in both categories were positioned within specific topologically associating domains (TADs), which were often differently regulated across different brain regions. These TADs were enriched in genes relevant for the physiological and behavioral observed changes. Our results suggest that chromatin structure coordinates diet-dependent transcriptional regulation.

29 Significance Statement

30

31 Mice fed with free-choice access to chocolate mixture become overweight and compulsive,
32 recapitulating what happens during obesity. For the first time, we correlated these physical and
33 behavioural changes with the transcriptome in the frontal cortex and the striatum, involved in the
34 hedonic "liking" associated to eating, and the hypothalamus, involved in the homeostatic regulation of
35 food intake. We detected two groups of genes: some transcript were strongly deregulated in term of
36 fold changes; while others were only subtly deregulated but were especially correlating with
37 measurements associated with body-weight and compulsivity. These genes were not randomly
38 distributed, but were positioned in chromatin domains, many of which rich in genes differentially co-
39 regulated across brain areas.

40

41 Introduction

42

43 Overeating, leading to obesity, is a serious concern in developed countries. Obesity is a major public
44 health threat leading to related diseases such as type II diabetes or atherosclerosis, and increasing
45 mortality (Di Angelantonio et al., 2016). The brain circuitry controlling eating in humans, and
46 participating in obesity development is modulated not only by homeostatic mechanisms regulating
47 food intake and energy expenditure, but also by reward, emotion/memory, attention, and cognitive
48 systems (Saper et al., 2002). Those mechanisms are non-homeostatic with regard to the body's
49 metabolism and energetic balance, and may lead to addictive-like behaviours such as compulsive-
50 overeating and inflexibility upon obesity development (Lee et al., 2012), being potent drivers of food
51 seeking (Kenny, 2011). The hypothalamus controls the energy-driven component of feeding
52 behaviour, while other regions, such as the frontal cortex and the striatum, control reward-related
53 aspects of food intake. These "metabolic" and "hedonic" brain areas need to be coordinated to allow a
54 proper ingestive behaviour and a balanced energy intake (Berthoud, 2012) and would be affected by
55 facilitated access to energy-dense and palatable food (Berridge et al., 2010). This coordination among
56 distant brain areas naturally uses multiple mechanisms, including cell-to-cell signalling and long-range
57 projections among different brain regions (Atasoy et al., 2012; Sweeney and Yang, 2017). However, it
58 also requires coordinated transcriptional regulation in various brain regions (Fenselau et al., 2017).
59 Much of the transcriptional response associated to overeating remains to be studied and the relational
60 patterns in gene expression changes among different metabolic and hedonic-related brain regions are
61 unknown.

62 One possibility would be that this regulation takes place in the context of topologically associated
63 domains (TADs). TADs are chromosomal domains evolutionarily conserved across tissues and
64 species. The genes present in TADs usually exhibit similar expression profiles (Dixon et al., 2012),
65 forming co-regulated clusters (Nora et al., 2012). Thus, we propose that the TAD structure
66 orchestrates the gene expression changes across different brain regions, allowing both a coordinated
67 and region specific response across different brain regions.

68 Here we explored the transcriptional profiles of frontal cortex, striatum, and hypothalamus, key brain
69 areas involved in overeating, in mice fed with free choice of a high palatable and energy-dense diet, a

70 model for overeating and unhealthy food consumption. We also measured physical and behavioral
 71 parameters in order to correlate them with transcriptional changes. Once we detected the genes
 72 changing their expression levels and correlating with body weight and behaviour, we explored their
 73 distribution on TADs across brain regions.

74 **Materials and Methods**

75 **Animals**

76 We used sixteen C57BL/6 (Charles River, France) female mice, of five weeks of age at the beginning
 77 of the experiments. Mice were housed in individually ventilated cages (IVCs) (Tecniplast, Italy) and
 78 PheCOMP cages (Multitake model, Panlab, Barcelona, Spain) in the Animal Facilities of the Barcelona
 79 Biomedical Research Park (PRBB, Barcelona, Spain, EU) in controlled laboratory conditions with the
 80 temperature maintained at $22\text{ }^{\circ}\text{C} \pm 1^{\circ}\text{C}$ and humidity at $55 \pm 10\%$ on a 12 hour light/dark cycle (lights
 81 off 20:00 hours). Food and water were available *ad libitum*. All animal procedures were performed in
 82 accordance with the [Author University] animal care committee's regulations.

83 **Diet induced weight gain**

84 All mice were habituated to their cages for one week provided with food and water *ad libitum*. Then,
 85 they were allocated to the group receiving standard chow (SC) or chocolate mixture (CM), balanced
 86 by body weight and housed individually in special metabolic cages (see below). During 8 weeks, SC
 87 mice had access to standard chow mouse diet (Trans 23 diet, Mucedola, Italy) providing 10,870
 88 KJ/Kg and CM mice had a free choice access to standard chow (SC) and to a chocolate mixture
 89 consisting of an equal weight of Mars®, Bounty®, Snickers® and Milka® prepared as homogenous
 90 food pellets following Heyne et al. protocol (Heyne et al., 2009). The chocolate provides 20,595 KJ/Kg
 91 with 52% of its energy from carbohydrate, 17% from protein and 24% from fat. The experimental
 92 schedule is shown in the Fig 1-1A-B.

94 **Feeding behavior analysis**

95 We used the PheCOMP multi-take metabolism cages (Panlab-Harvard Instruments, Barcelona,
 96 Spain) to obtain fine grain data for individualized mouse including the grams of food consumed, the
 97 number of meal events and the temporal distribution of the feeding bouts in a continuous recording

(Espinosa-Carrasco et al., 2018). The system contains two foods dispensers. SC mice received standard rodent chow (SC) in both whereas CM mice had one dispenser with standard chow and the other with chocolate-mixture. The location of each dispenser was counterbalanced between cages. From the quantitative data obtained by the PheCOMP cages, we calculated the energy intake, measured by multiplying the known energy content (kJ/g) of individual foods by the amount of food consumed. The eating rate (kJ/sec) was obtained using the COMPULSE software (Panlab-Harvard Instruments, Barcelona, Spain).

Test battery for the study of compulsivity

Tests were performed in a set order designed to minimise the effect of testing on following tests and with sufficient inter-test intervals to provide an opportunity for the mouse to re-establish its previous feeding behaviour and relieve any test-induced stress. The free-choice diet was suspended only during the “limited access to chocolate mixture” and “CM adulteration” tests (five days in total). Thereafter the initial diet was reintroduced during six days, before the animals were sacrificed.

Temporally limited access to chocolate mixture (CM)

We used limited access to CM to measure the binge-like behaviour, as readout of compulsion induced by restricted access to the preferred food. Standard chow and water were provided *ad libitum*. Access to CM was restricted to 1 hour per day during the middle of the light phase for 3 consecutive days (Heyne et al., 2009). SC mice were also provided with CM during this hour. In CM mice, we compared the CM consumed during the period of access with the CM consumed in non-limited conditions. This value was obtained as the mean of 3 days of CM intake during the previous week of the battery of tests, at the same time (between 14:00 and 15:00).

Chocolate mixture adulteration

Chocolate adulteration provides information concerning flexibility of food intake under aversive conditions. Mice were given a free choice between standard chow (SC) and a pellet of the chocolate

125 mixture (CM) adulterated with quinine hydrochloride (SIGMA-Aldrich) 1g/kg food to give it a bitter
 126 taste. According to (Heyne et al., 2009) flexible mice will avoid or decrease the intake of CM.

127

128 **Nestlet shredding test and grooming behaviour**

129 Mice were given a cotton square (Ancare, New York, USA) in their home cage under food-deprived
 130 conditions (water was still provided ad libitum) for 30 minutes during the middle of the light phase. The
 131 cotton was weighed before and after the test to provide a measure of nesting ability based on the
 132 amount of material the mouse had used to nestlet (Deacon, 2006). The grooming behaviour was
 133 recorded (Biobserve, Bonn, Germany) and the number and length of events were quantified by an
 134 investigator blind to the experimental condition.

135 **Statistical analysis of behaviour**

136 Repeated measures ANOVA was used for the comparison of the body weight evolution across the
 137 experimental weeks. Differences were considered significant at $P < 0.05$. All results are expressed in
 138 mean \pm SEM. The statistical analysis was performed using the Statistical Package for Social Science
 139 program SPSS® 12.0 (SPSS Inc, Chicago, USA).

140 **Gene expression**

141 Frontal cortex, striatum and hypothalamus, from SC and CM groups, were dissected upon completion
 142 of an 11-day test battery and total RNAs extracted with *Qiagen's RNeasy mini kit* for hybridization with
 143 Agilent's gene expression arrays (*SurePrint G3 Mouse GE 8x60K array v1*).

144 Cyanine-3 (Cy3) labelled cRNA was prepared from 100ng of total RNA using the *LowInputQuick Amp*
 145 *Labelling kit Agilent 5190-2305* according to the manufacturer's instructions, followed by *RNAeasy*
 146 column purification (*QIAGEN*, Valencia, CA). Dye incorporation and cRNA yield were checked with
 147 the *NanoDrop ND-1000* Spectrophotometer.

148 After fragmentation, 600 ng of labelled cRNA from each sample was hybridised in *in situ* hybridisation
 149 oven (*Agilent*) for 17 h at 65°C and washed during 1 min at room temperature in *Gene Expression*
 150 *Wash Buffer 1 (Agilent)* and 1 min at 37 °C with *Gene Expression Wash buffer 2 (Agilent)*.

151 Scanned on an *Agilent G2539A* scanner at 3 um resolution and 100% PMT. The intensity data of
 152 each individual hybridization were extracted and the quality was assessed with the *Feature Extraction*

153 *software 10.7 (Agilent)*. The intensity data of each individual hybridization were extracted and the
 154 quality was assessed with *the Feature Extraction software 10.7 (Agilent)*.

155 **Bioinformatic analysis**

156 Intensity values were imported into R using the *limma* function *read.maimages* (Ritchie et al., 2015).
 157 Samples were background corrected and normalised using the *normexp* normalization: a convolution
 158 of normal and exponential distributions is fitted to the foreground intensities using the background
 159 intensities as a covariate, and the expected signal given the observed foreground becomes the
 160 corrected intensity (Shi et al., 2010). This results in a smooth monotonic transformation of the
 161 background subtracted intensities such that all the corrected intensities are positive. Background has
 162 been computed from the 95% percentile of the intensity of the negative control probes on each array,
 163 keeping probes that are at least 10% higher than the negative controls on at least four arrays
 164 (because there are four biological replicates). Values for within-array replicate probes are replaced
 165 with their average to have a “one value - one gene” matrix. We fitted a linear model by using both
 166 brain areas and diet as covariates, blocking for the mouse for taking into consideration the same
 167 provenance of the three brain regions. The values of the moderated t-statistics were corrected for
 168 multiple-testing using the Benjamini-Hochberg correction (Benjamini and Hochberg, 1995).
 169 Multi-Dimensional Scaling was performed using the *limma plotMDS* function. The distance between
 170 each pair of samples is the root-mean-square deviation for the top 500 genes (selected for each pair
 171 of samples). Distances on the plot can be interpreted as leading log2-fold-change, meaning the
 172 typical (root-mean-square) log2-fold-change between the samples for the genes that distinguish those
 173 samples (Ritchie et al., 2015).

174 We used the *matplotlib_venn* python module and *gplots* R package (Warnes et al.) for drawing the
 175 overlaps and we assessed the significance of the overlaps with the exact Fisher test.

176 Probes were converted to *entrez* identifier by using the *biomaRt* package (Durinck et al., 2009) and
 177 gene ontology and pathway analysis were performed with the *clusterProfiling* package (Yu et al.,
 178 2012).

179 **Correlation with behavioural data**

180 We correlated each of the gene expression microarray intensities with body weight and the
 181 behavioural data measured in our mice. Since we were interested both in the final body weight and in

its increase, we performed a PCA with these two variables and extracted for each mouse the resulting values of principal component 1 to combine those variables in a unique measurement (Fig 3-1 C). Similarly, we combined through PCA six other variables to have a unique measurement of compulsivity: grooming; nesting; the energy rate from day 1, 2, 3; and from the quinine adulteration test (Fig 3-1 B-F). The variables within these two sets were correlated with the gene expression values. After this analysis, we finally selected five parameters to correlate: two set of PC1 values—body weight and compulsivity—and three behavioural measurements inflexibility, energy intake, and eating rate. We selected for further analyses only the correlating microarray probes changing between SC and CM mice at least by 10% and whose adjusted p-value upon z-fisher correction was lower than 0.05.

Testing if the gene expression fold changes fitted the TAD segmentation profile

We mapped genes with the Entrez identifiers using *BiomaRt* (Ensembl archive May, 2017) to the TAD borders as defined in Dixon et al. (Dixon et al., 2012) for cerebral cortex. TADs borders were defined using a Directionality Index method (Dixon et al., 2012). To test whether there was agreement between the differential expression profile in the three studied brain regions and the TAD segmentation we have performed three types of *in silico* permutation testing (Fig 4-1A). For the tests, we selected only the genes that were clustered within TADs containing five or more genes. In the first approach genes were re-assigned to random TADs, however maintaining original gene numbers in particular TADs and using only the genes, which were within TADs in the original case. Second type of permutation involved changing borders of TADs by permuting the collection of pairs of: TAD's length + distance to the next TAD downstream, maintaining the original gene localizations on chromosomes. Each type of permutations was made 1000 times and each time Kruskal-Wallis test was performed. Finally, the H-statistics from original data were compared with the averaged values from the permuted H-statistics as well as compared with the decreasing rank of the permuted H-values.

Selecting regulated TADs

We defined as *regulated* TADs, the TADs with a significantly higher number of DE or correlating genes across the three brain areas. Once mapped these genes to TADs, we used the *PowerLaw* R

212 Package to check what kind of heavy-tail distribution the number of regulated genes per TAD
213 approximated. We compared *Poisson*, *Power-law*, *exponential*, and *log normal*, finally selecting the
214 *log normal* to select the TADs whose probability of finding by chance another TAD with a higher
215 number of regulated genes was lower than 0.05.

216 **Testing if responsive genes are co-regulated within regulated TADs**

217 To test whether the DE and correlating genes contained in *regulated* TADs clustered according to
218 their fold change (e.g. up-regulated genes in certain TADs, down-regulated genes in other TADs), we
219 performed a permutation test. We considered as *responsive* genes each gene DE or correlating. Our
220 rationale was that in case of an equal number of upregulated and downregulated genes, if genes
221 were randomly distributed along TADs, the difference between the number of up-regulated and the
222 number of downregulated genes had to be on average 0, while if the contrary were true, we would
223 expect both TADs with a positive difference (more up-regulated genes), and with a negative
224 difference (more down-regulated genes). Therefore, first we computed the absolute value of the
225 differences between the number of upregulated and downregulated *responsive* genes for each TAD,
226 and then we calculated the average observed deviation per *regulated* TAD, in each brain region. We
227 then randomly shuffled 1000 times the *responsive* genes maintaining the number of genes per TAD
228 fixed and recalculated the average deviations in each region. The *p-value* was given by summing how
229 many times we observed by chance (in the permuted datasets) a higher deviation than what observed
230 in our data $+1$, divided by the number of permutation $+1$. Using only *responsive* genes for re-
231 assigning genes to regulated TADs, we assured that our results were significantly different than what
232 expected by chance for a given pattern of fold changes. For instance, if upregulated genes among
233 responsive were naturally more numerous, we would expect higher deviation from zero even if these
234 genes were randomly distributed across *regulated* TADs, and therefore we took into account this
235 higher probability of re-assigning an up-regulated gene in our permutations.

236 All the code for the bioinformatic analysis is reported as Supplementary Data 1. Analyses were
237 performed with R version 3.5.0 (2018-04-23). Platform: x86_64-apple-darwin15.6.0 (64-bit) .Running
238 under: macOS High Sierra 10.13.4.

239 **Contact map**

240 Contact-map was created using visualization tool *DiffTAD* (Zaborowski and Wilczynski, 2016) and the
241 chromatin contacts data (TAD borders) come from the Hi-C experiment performed by Dixon et al.
242 (Dixon et al., 2012).

243

244 **Data availability**

245 To be added after acceptance to respect double blindness

246

247 Results

248 Free access to chocolate induces overweight and compulsive overeating

249 To investigate the effect of our experimental design on the brain transcriptome we performed in vivo
250 experiments and took measurements from 8 mice given free access to chocolate mixture diet and
251 standard chow (CM mice; Fig 1A-B) and 8 mice receiving standard chow (SC mice). CM mice
252 increased their body weight upon chocolate mixture access (repeated measures ANOVA, $F_{1,14} =$
253 19.30; $P=0.001$), whilst SC mice did not significantly change their weight along the experiment (Fig
254 1C). There is a slight increase of body weight in both experimental groups during the first weeks,
255 possibly reflecting the normal growth curve, but after 8 weeks of free chocolate mixture access, body
256 weight was significantly higher in the CM group only. We also measured behavioral parameters in
257 order to correlate them with transcriptional changes. The test battery included limited access to the
258 chocolate, quinine test, nest building test (Fig 1B). Moreover, we monitored in both groups the energy
259 intake (KJ/Kg), eating rate (mg/s), food intake during limited access and quinine test (g/Kg of body
260 weight/h), and grams of cotton in the nest building test, and the grooming time (s). We then checked if
261 these measurements were able to separate SC from CM mice using Principal Component Analysis
262 (Fig 1D). Interestingly, behavioural variables contributed to the separation of SC and CM mice along
263 PC1, as much or even more than body weight related variables, suggesting that body weight changes
264 in CM mice are accompanied by strong behavioural changes. Raw behavioural data are accessible in
265 Extended Data 1-1.

266 Transcriptional responses can be clustered by brain region and diet

267 We performed a microarray experiment to assess the effect of our experimental design on the
268 transcriptional profile of three brain areas: the frontal cortex, the striatum, and the hypothalamus (4
269 animals per group). Multidimensional scaling showed that the first leading dimension is mainly
270 separating the hypothalamus from the frontal cortex and the striatum, indicating that the hypothalamic
271 transcriptional profile diverges significantly from that of the striatum and frontal cortex, while the
272 second dimension is further separating the frontal cortex from the striatum, and, less perfectly, SC
273 from CM mice (Fig 2A).

274 When assessing the *CM-SC* contrast with a linear model, we found 662 differentially expressed (DE)
 275 genes upon CM diet in the frontal cortex, 142 in the striatum and 44 in the hypothalamus upon setting
 276 specific threshold of fold-changes and adjusted p-value (Fig 2B-C). Two thirds of the striatal and half
 277 of the hypothalamic DE genes significantly overlapped with frontal cortex DE genes. Instead, we
 278 found no overlap between the striatum—part of the reward system—and the hypothalamus—involved in
 279 homeostatic energy intake. Volcano plots of the overall transcriptomic changes showed that frontal
 280 cortex genes presented the higher absolute fold changes, followed by the striatum, while
 281 hypothalamic genes showed modest fold changes, indicating that weight gain led to a wider and
 282 stronger response (in term of differential expression) in the frontal cortex (Fig 2C). Summary tables for
 283 the differential expression analyses are reported as Extended data 2-1, 2-2, and 2-3.

284 **Most of the genes highly correlating with behavioural variables show subtle** 285 **expression changes**

286 To determine which transcriptional changes were correlating with the physical/behavioural alterations,
 287 we tested the correlation of the overall gene expression changes (not only those DE) with the five
 288 parameters that mainly contributed to the observed inter-sample variance (see *Methods*). These
 289 parameters included both composite measurements: body weight (Fig 3-1A), and compulsivity (Fig 3-
 290 1B); and direct measurements: inflexibility (Fig 3-1C), total food intake, and eating rate (Fig 3-1D and
 291 Fig 3-1E).

292 In each brain region, we identified sets of genes significantly correlating with specific
 293 behavioural/physical variables (Fig 3A). The frontal cortex showed the highest number of genes
 294 correlating with total food intake, body weight and inflexibility and, to a lesser extent, compulsivity and
 295 eating rate. In the hypothalamus, we detected a high number of genes correlating with body weight,
 296 while in the striatum we found a lower number of correlating genes—mostly correlating with inflexibility.
 297 Most of the genes highly correlating with behavioural variables showed subtle expression changes
 298 (average absolute log2FC of about 0.2-0.4; Fig 3B and Fig. 3-2 to Fig 3-6). When plotting the log2FC
 299 as a function of the Spearman “rho”, we observed a high correlation with phenotypic variables for
 300 genes changing less than 1.5 times (rho range: 0.27-0.86), and a low correlation for genes changing
 301 more than 1.5 times (rho range: 0-0.25).

302 Instead, only few differentially expressed (DE) genes were significantly correlating with behaviour or
 303 body weight, as demonstrated by the low overlaps between DE genes and correlating genes (Fig 3C).
 304 The most relevant overlaps were found between hypothalamic DE genes correlating with body weight
 305 (31%), and frontal cortex DE genes correlating with inflexibility (13.7% of correlating genes). Overall
 306 79% of frontal cortex DE genes, 96% of striatum DE genes, and 66% of hypothalamic genes were not
 307 correlating with any of our studied variables, indicating that DE and correlating genes are two different
 308 categories of regulated genes.

309 Contrary to DE genes, which were shared across brain regions with quite high overlap (frontal cortex
 310 DE genes with striatal and hypothalamic DE genes), genes correlating with a given phenotypic
 311 variable were not the same across the three brain regions (Fig 3C) with low overlaps both *intra*-
 312 (among phenotypical variables) and *inter*- brain region. This suggests the need of activation of both
 313 common and region specific transcriptional programs in each brain area, for each phenotypic change
 314 to occur. Two exceptions were the overlap of genes correlating with total intake and inflexibility in the
 315 frontal cortex (46%) and genes correlating with inflexibility and compulsivity in the striatum (63%, Fig
 316 3C).

317 **Transcriptional changes affect both common and region specific molecular** 318 **pathways**

319 We then investigated the molecular pathways (Fig 3-7A for Reactome and 8B for KEGG), and gene
 320 ontologies (Fig 3-7C) enrichment of both DE genes (changing their expression more than 1.5-2
 321 times), and genes significantly correlating with phenotypic variables (mainly showing more modest
 322 log2 FCs of 0.2-0.4) in the three brain areas.

323 In the hypothalamus DE genes were mainly enriched in Reactome's "Olfactory Signaling pathways"
 324 (Fig 3-7A), KEGG's "Olfactory transduction" (Fig 3-7B) and GOs "Olfactory receptor activity" and
 325 "Sensory perception of smell" (Fig 3-7C). Hypothalamic genes correlating with inflexibility were mainly
 326 enriched in the Reactome "Endosomal/Vacuolar pathway", and the metabolic pathway "Translocation
 327 of GLUT4 to the plasma membrane" (Fig 3-7A) categories and several GOs related to the metabolism
 328 of fatty acids and sugars such as lactonase, hydrolase, mannosidase, and esterase activity (Fig 3-
 329 7C). Finally, hypothalamic genes correlating with body weight showed enrichments mainly in
 330 epigenetic/chromatin pathways, indicating they are tightly regulated at the transcriptional level.

Frontal cortex DE genes, similarly to hypothalamic ones, were also enriched in “Olfactory transduction” and “Taste transduction” pathways (Fig 3-7B), together with “Olfactory receptor activity” and “Sensory perception of chemical stimulus”. Frontal cortex genes correlating with inflexibility were similarly enriched in “Olfactory transduction” (Fig 3-7B) and “Olfactory receptor activity” (Fig 3-7C), consistently with the overlap between *inflexibility* genes and frontal cortex DE genes (Fig 3C). Finally, frontal cortex genes correlating with compulsivity were enriched in the immunity pathway “Alpha-defensins” (Fig 3-7A). Taken together, the results indicate that genes belonging to olfactory transduction related pathways are commonly deregulated in both the hypothalamus and the frontal cortex, where part of these genes is also highly correlating with inflexibility.

Regarding the striatum, genes correlating with inflexibility and compulsivity shared enriched categories, as expected by their high overlap of 63% (Fig 3C), suggesting that compulsivity and inflexibility are connected processes in the striatum, involving pathways such as “Alcoholism” (Fig 3-7B) and chromatin pathways mainly related to gene silencing (Fig 3-7C). Other striatal genes such as genes correlating with eating rate were enriched in “Glyoxylate and dicarboxylate metabolism” (Fig 3-7B), while genes correlating with body weight with GOs “Mitochondrial membrane” (Fig 3-7C). Finally, genes correlating with total intake in the striatum were both enriched with nuclear/transcriptional pathways and immune pathways related with leukocytes (Fig 3-7A and 3-7C). Summary tables for the enrichment analysis are reported as Extended data 3-1, 3-2, and 3-3.

Gene expression changes are organised within regulatory domains

The analyses above showed that the transcriptional responses involve both commonly regulated and brain-region specific genes. Recently published results showed that genes lying within the same TADs have stronger correlation in expression than genes separated by TAD borders (Ramírez et al., 2018) and that actively expressed open chromatin regions are spatially separated from inactive ones (Rennie et al., 2018). However, it has not been shown whether changes in gene expression caused by a stimulus such as the different diets before the test battery in our experimental design would conform to the TAD structure as well or would be TAD-independent. Also, it has not been shown that such changes would occur in the mammalian brain. Therefore, to verify if such regulation could take place, we tested whether the genes conformed to a common regulatory domain (TAD) structure in each of the investigated brain areas. To this purpose, we used the segmentation of mouse

chromosomes into 1519 TADs as determined by Dixon et al. (Dixon et al., 2012) based on Hi-C experiments in cortical tissue (Extended data 4-1).

We compared the distributions of all gene expression fold changes within TADs with the Kruskal-Wallis test. The distributions of fold changes across TADs were significantly different: in all brain areas the p-values of the Kruskal-Wallis test were lower than 10^{-37} (Fig 4-1A). To assess the robustness of these significant p-values we performed two different permutation tests. First, we re-assigned *in silico* genes to TADs, therefore completely changing the published topological organization (Dixon et al., 2012). This led to a dramatic drop of the H-statistics (for instance in the hypothalamus from $H = 1991$, $p\text{-val} = 6.7E^{-47}$ to average H of 1000 permutations = 1157, $p\text{-val} = 0.5$), indicating that our results were specific for the specific TAD structure in the brain. Secondly, we applied a subtler permutation where we re-shuffled randomly TAD boundaries while keeping the original gene positions. As expected, in this case p-values were less severely affected than in the previous permutation (e.g. for hypothalamus, decrease from $H = 1991$, $p\text{-val} = 6.7E^{-47}$ to average H-statistics of the 1000 permutations $H = 1665$, $p\text{-val} = 2.1E^{-27}$) (Fig 4-1A).

We also investigated if the distribution of the *rho* values for each of our phenotypical variables (body weight, compulsivity, inflexibility, energy intake and eating rate) agreed with the TADs segmentation pattern. Again, the distribution of *rho* values was not random across TADs, indicating that the correlation values were not uniformly distributed but tended to cluster in agreement with the TAD structure (e.g. for hypothalamus, eating rate, $H = 2514$, $p\text{-val} = 6.23 E^{-102}$, as compared to average of the 1000 permutations: $H = 1154$, $p\text{-val} = 0.5$) (Fig 4-1B).

Overall, these analyses suggest that both gene expression changes between SC and CM groups and correlation values between genes and phenotypic variables occur in conformity with the brain TAD structure.

A high number of TADs were simultaneously co-regulated across the three brain regions

To determine if TADs were involved in the coordination of region specific transcriptional responses, we analysed all the TADs containing regulated genes—both DE and correlating—for each brain area. These TADs overlapped widely across the three brain regions, with 502 TADs shared in at least two brain regions, and 161 across the three brain regions (Fig 4A). Concordant to its higher and wider

transcriptional response, the frontal cortex contained the highest number of region specific TADs. However, when looking at the number of genes per TADs, most of the regulated genes were contained in the same TADs across brain areas. This held true also for the frontal cortex, in which even though we found a higher number of region specific TADs, most of the regulated genes mapped to common TADs (Fig 4-2A).

The number of regulated genes per TAD followed a heavy-tailed distribution with hundreds of TADs containing only one or few regulated genes and a long tail with few TADs highly enriched in regulated genes (Fig 4B). This tendency was significant, as verified by permutation testing.

Considering the overall area of this distribution of TADs as 1, we named *regulated TADs* (n=37; bars on the right of the dashed line in Fig 4B) those in the tail on the right of the graph (cut off for the area of 0.05). These TADs contained more than 10 genes co-regulated either within a specific brain region and/or among regions. Interestingly, all *regulated TADs* contained genes regulated in at least 2 different brain areas, and more than 90% of them contained genes regulated across all the three studied brain areas (Fig 4C).

In the hypothalamus, genes correlating with body weight were mainly localised in *regulated TADs* suggesting that genes in these TADs are needed for body weight regulation (Fig 4D). In the frontal cortex, regulated TADs showed the highest enrichments in DE genes, and in genes correlating with inflexibility, body weight, and total intake. In the striatum *regulated TADs* were also enriched in genes correlating with inflexibility (Fig 4D).

We detected transcriptional co-regulation both within and across brain regions. Within brain regions, many regulated TADs contained at the same time genes correlating with different phenotypical variables (e.g. *regulated TADs* containing *compulsivity* genes and *inflexibility* genes in frontal cortex). Across brain regions, regulated TADs contained genes correlating with phenotypical variables in at least 2 or 3 brain regions (e.g. *inflexibility* genes or *body weight* genes across the three brain regions, Fig 4E).

Since TADs would provide the epigenetic environment for co-expression of groups of genes, up-regulated and down-regulated genes may cluster separately in certain *regulated TADs*. In fact, differences between up- and down-regulated genes per TAD often deviated from zero (Fig 4-2B, left side). These deviations were higher in frontal cortex with a group of *regulated TADs* containing mainly up-regulated genes, and another group containing mainly down-regulated genes. In the

419 hypothalamus, almost the all *regulated* TADs contained down-regulated genes while the striatum
420 showed much lower deviations in the number of up- and down-regulated genes per TAD (Fig 4-2B,
421 left side). These deviations were significant for the frontal cortex (mean difference per TADs between
422 the number of up-regulated and down-regulated genes of 3.78, p-value=0.02), and for the
423 hypothalamus (mean deviation of 2, p-value=0.002), but not for the striatum (mean deviation of 1.14,
424 p-value=0.7). See *Methods* for a detailed explanation of the permutation test used. These results
425 indicate that in both the frontal cortex and the hypothalamus, responsive genes distribute accordingly
426 to their fold-change along the *regulated* TADs, showing intra-TAD co-regulation.

427 Interestingly, over 70% of *regulated* TADs contained genes up-regulated in the frontal cortex, and
428 down-regulated in the hypothalamus, supporting the idea that in some cases TADs are regulated
429 differently depending on the brain area. Each *regulated* TAD contained genes correlating to different
430 phenotypical variables or DE genes (Fig 4-2B, right side), suggesting that these functions could be
431 finely regulated in space and time thanks to the TAD organization.

432 One example of a TAD containing co-regulated genes is TAD 624 (Fig 4F), with a group of genes
433 mainly up-regulated in the frontal cortex, mainly down-regulated in the hypothalamus, and with less
434 evident intra co-regulation in the striatum (clusters of blue or red bars).

435

Discussion

In this work, we were interested in understanding the mechanisms of transcriptional responses comparing mice receiving two different diet regimes—standard chow versus energy-dense, free choice diet— in brain regions involved in the homeostatic and hedonic control of feeding behaviour.

The transcriptional profile in the frontal cortex, striatum and hypothalamus was modified consistently with the transcriptional associated domain (TAD) segmentation pattern. We detected two levels of transcriptional regulation: a switch-like regulation with differentially expressed (DE) genes changing over 1.5 fold; and a “fine-tuned” gene regulation, with subtler expression changes, but highly correlated with body weight gain and behavioural changes. Even though the modulation of many genes was brain-region specific, mapping of the transcriptional response at the TAD level revealed many TADs that were responsive (contained DE or correlating genes) in more than one brain area. Interestingly, the 37 TADs containing the highest number of regulated genes were common across brain areas. In most cases, genes in a given TAD were up-regulated in one brain area and down-regulated in another, indicating the importance of the TAD structure for achieving both a coordinated and brain-area specific response.

We conclude that the conserved TAD structure from Dixon et al. (Dixon et al., 2012), participates in orchestrating gene regulation within and among brain regions controlling energy intake and reward, probably allowing a coordinated homeostatic and hedonic response.

Different physical and behavioral parameters correlate with transcription, suggesting a coordinated and specific response across brain areas

Our free-choice paradigm promoted body weight gain and meal pattern and behavioural changes in mice. In our microarray experiment, the hypothalamus showed a remarkably different transcriptional response compared to the striatum and the frontal cortex as revealed by multidimensional scaling. This would support the different role of the hypothalamus, which controls the homeostatic regulation, from the frontal cortex and the striatum, which control the hedonic regulation of appetite. This first approach used classical differential gene expression analyses that only consider those gene expression changes satisfying specific criteria of fold change and within-group variance (Phipson et

al., 2016). However, thanks to our experimental design, we could directly test the correlation of gene expression with body weight and behavioural measurements. In fact, since we collected the brain samples six days after the test battery, our observed gene expression profiles might not only be the result of the diet (SC or CM), but also of the interaction of the chronic effect of the diet regime with the battery test performed (for example a gene could be differentially expressed when comparing the CM and the SC groups but only after the two groups undergo the test battery). Of course our experimental design does not allow to disentangle the respective contribution on gene expression of the diet, the behavioral battery, or their interaction, but that goes beyond our aim. What we can state is that whether an interaction between the effects of the diet and the behavioural battery occur or not, in both cases the observed differences would be triggered by the different diet regimes, since the test battery is performed in the exact same way for the two groups, and therefore would cancel out when computing the *CM-SC* contrast. This original approach revealed genes highly correlated with the phenotype, that otherwise would have been filtered out for having too subtle absolute differential expression fold changes and/or too high intra-group variability. To reduce the biases related to single variables, in the case of variables characterised by multiple types of measurements, we correlated the first principal component instead of single variables. For example, compulsivity is a complex behavioural domain that is reflected in increased grooming, impaired nesting behaviour, increased overeating (energy intake) across days, especially when access to energy dense diet is restricted, and inflexible behaviour in the quinine adulteration test. We speculate that genes correlating directly to a given phenotypical variable are responding to our experimental design even if in a subtler way. Remarkably, the number of correlating genes varied significantly among brain areas in accordance with their distinct biological role in feeding behaviour regulation. For example, *inflexibility* correlated with hundreds of genes in the frontal cortex and the striatum, the brain areas that are mainly responsible for this behaviour, but not in hypothalamus, whose genes mainly correlated with *body weight*. This fits with the hypothalamic role in the homeostatic control of energy intake (Sisley and Sandoval, 2011).

Given the importance of this finding, we included both DE and correlating genes in our pathway analysis. Among the most significant pathways we found GO enrichment in "Olfactory signalling related processes" when analysing DE genes in the frontal cortex and in the hypothalamus, and genes correlating with inflexibility in frontal cortex. There are more than 1000 olfactory receptor genes

495 in the mouse genome, that encode G-protein coupled receptor that work as chemical sensors in the
496 brain (Garcia-Esparcia et al., 2013). Interestingly, among the natural ligands of those olfactory
497 receptors are fatty acid derivatives (Sartorius et al., 2015) that would be increased by our chocolate
498 mixture diet. Other categories found consistently enriched are related to the immune response. For
499 instance, *compulsivity* genes in frontal cortex were enriched in defensins and total intake genes in the
500 striatum in leukocyte-related pathways. In line with this, it is known that obesogenic food can also
501 induce neuroinflammation (Beilharz et al., 2015).

502 Moreover, according to the role of the striatum in reward and addiction, we found enrichment in the
503 "Alcoholism" pathway for striatal genes correlating with inflexibility and compulsivity (Volkow et al.,
504 2013). The high overlap between striatal genes correlating with inflexibility and compulsivity suggests
505 that the processes leading to compulsive and inflexible behaviours are similar in the striatum. In this
506 region, genes correlating with eating rate were enriched in "Glyoxylate and dicarboxylate metabolism",
507 and genes correlating with body weight with "Mitochondrial membrane". In the hypothalamus, we
508 found genes involved with inflexibility that were enriched in pathways involved in the metabolism of
509 glucose and fatty acids. For example, we detected an enrichment for the translocation of the glucose
510 transporter GLUT4 on the plasma membrane, a pathway normally activated by insulin to allow the
511 uptake of glucose from the bloodstream (Muretta and Mastick, 2009).

512 Finally, many categories involved in chromatin, epigenetic and transcriptional regulation were
513 specifically enriched when looking at genes correlating with body weight in the hypothalamus and
514 compulsivity and inflexibility in the striatum. This suggests that these processes might be
515 epigenetically regulated in these brain areas.

516 **TADs orchestrate the brain-area specific response**

517 In our dataset, some groups of genes, such as genes DE in frontal cortex and hypothalamus, genes
518 correlating with inflexibility in frontal cortex, and genes correlating with compulsivity and inflexibility in
519 the striatum were highly overlapping and shared biological pathways such as "Olfactory
520 Transduction". However, we also detected many region-specific genes, leading to region-specific
521 pathway enrichments. We wondered how region-specific mechanisms would co-exist with the need to
522 coordinate different responses both intra- and inter- brain areas.

Therefore, we explored the distribution of regulated genes along the chromosomes to identify potential regulatory mechanisms leading to the observed expression profiles. We found that both DE genes and subtly regulated genes correlating with phenotypic and behavioural variables were not randomly distributed throughout the genome, but organised in genomic clusters, the TADs. The non-random organization of genes along eukaryotic chromosomes is well established and plays a role in the coordination of gene expression, and thus might have a functional role at the transcriptional stage. To detect the most relevant genomic regions responsive to our experimental design in brain, we focused our analysis on the TADs with the highest number of DE genes or genes correlating with some specific behavioural variables across brain areas (what we named *regulated* TADs). All *regulated* TADs contained genes responsive across brain areas, and correlating with different phenotypical variables, indicating that they are important for the regional co-regulation in the brain, and for the coordination of the different responses initiated in our two groups of mice. Consistently with the homeostatic role of the hypothalamus, we found that the majority of the *regulated* TADs containing hypothalamic genes, contained genes correlating with body weight. Similarly, the frontal cortex or striatum genes contained in *regulated* TADs were correlated with inflexibility, in agreement with the role of these brain regions in the hedonic responses to food.

We observed that the DE or correlating genes contained in *regulated* TADs tended to have expression changes of the same sign, supporting the idea that TADs provide the epigenetic environment for co-expression of groups of genes (Tanay and Cavalli, 2013). Interestingly, many *regulated* TADs show a different direction of regulation depending on the brain area (the same TAD could contain for example genes mainly upregulated in one brain area, and mainly downregulated in another).

The fact that the same TADs contain genes co-regulated *within* a brain area and regulated in different directions *across* brain areas, might be surprising at first, but is consistent with the “epigenetic plasticity” model, for which a permissive or “plastic” chromatin state activate regulatory programs (Flavahan et al., 2017). Based on our findings, we could speculate that these *regulated* TADs are thus the genome regions of highest epigenetic plasticity.

550 Conclusions, limitations and future direction

551 Our results support the hypothesis that the homeostatic and hedonic control of eating behaviour could
552 be coordinated thanks to TADs inducing a specific and coordinated transcriptional changes both *intra*-
553 and *inter*- brain areas (Fig 5). Of course, we cannot discard that the test battery itself affects the
554 transcriptional profile; nonetheless the changes should affect similarly the CM group and the SC
555 group.

556 Also, we cannot rule out the possibility that our experimental design could affect the TAD structure,
557 but given the fact that the domain structure is mainly stable (Barutcu et al., 2015), we assumed that
558 the TAD boundaries remained intact. Expectedly, permuting those borders just slightly increased the
559 p-values associated with the Kruskal-Wallis test (but statistical significance was preserved). Finally,
560 brain regions contain different cell types and we observe only the “final” averaged effect. Single-cell
561 RNA sequencing or separation tagged cell populations could be used to assess which are the main
562 cell subtype which are responding to the energy-dense diet. Our findings warrant future studies
563 directly aimed to detect changes in the 3D genome organization upon energy-dense diet.

564

566 **References**

-
- 567
568 Atasoy D, Betley JN, Su HH, Sternson SM (2012) Deconstruction of a neural circuit for hunger. *Nature*
569 488:172-177.
- 570 Barutcu AR, Lajoie BR, McCord RP, Tye CE, Hong D, Messier TL, Browne G, van Wijnen AJ, Lian JB,
571 Stein JL, Dekker J, Imbalzano AN, Stein GS (2015) Chromatin interaction analysis reveals
572 changes in small chromosome and telomere clustering between epithelial and breast cancer
573 cells. *Genome biology* 16:214.
- 574 Beilharz JE, Maniam J, Morris MJ (2015) Diet-Induced Cognitive Deficits: The Role of Fat and Sugar,
575 Potential Mechanisms and Nutritional Interventions. *Nutrients* 7:6719-6738.
- 576 Benjamini Y, Hochberg Y (1995) Controlling the False Discovery Rate: A Practical and Powerful
577 Approach to Multiple Testing. *Journal of the Royal Statistical Society Series B*
578 (Methodological) 57:289-300.
- 579 Berridge KC, Ho CY, Richard JM, DiFeliceantonio AG (2010) The tempted brain eats: pleasure and
580 desire circuits in obesity and eating disorders. *Brain Res* 1350:43-64.
- 581 Berthoud HR (2012) The neurobiology of food intake in an obesogenic environment. *The*
582 *Proceedings of the Nutrition Society* 71:478-487.
- 583 Deacon RM (2006) Assessing nest building in mice. *Nat Protoc* 1:1117-1119.
- 584 Di Angelantonio E et al. (2016) Body-mass index and all-cause mortality: individual-participant-data
585 meta-analysis of 239 prospective studies in four continents. *Lancet* (London, England)
586 388:776-786.
- 587 Dixon JR, Selvaraj S, Yue F, Kim A, Li Y, Shen Y, Hu M, Liu JS, Ren B (2012) Topological Domains in
588 Mammalian Genomes Identified by Analysis of Chromatin Interactions. *Nature* 485:376-380.
- 589 Durinck S, Spellman PT, Birney E, Huber W (2009) Mapping Identifiers for the Integration of Genomic
590 Datasets with the R/Bioconductor package biomaRt. *Nature protocols* 4:1184-1191.
- 591 Espinosa-Carrasco J, Burokas A, Fructuoso M, Erb I, Martin-Garcia E, Gutierrez-Martos M, Notredame
592 C, Maldonado R, Dierssen M (2018) Time-course and dynamics of obesity-related behavioral
593 changes induced by energy-dense foods in mice. *Addiction biology* 23:531-543.
- 594 Fenselau H, Campbell JN, Verstegen AMJ, Madara JC, Xu J, Shah BP, Resch JM, Yang Z, Mandelblat-
595 Cerf Y, Livneh Y, Lowell BB (2017) A rapidly acting glutamatergic ARC→PVH satiety circuit
596 postsynaptically regulated by [alpha]-MSH. *Nature neuroscience* 20:42-51.
- 597 Flavahan WA, Gaskell E, Bernstein BE (2017) Epigenetic plasticity and the hallmarks of cancer.
598 *Science* (New York, NY) 357.
- 599 Garcia-Esparcia P, Schlüter A, Carmona M, Moreno J, Ansoleaga B, Torrejón-Escribano B, Gustincich
600 S, Pujol A, Ferrer I (2013) Functional Genomics Reveals Dysregulation of Cortical Olfactory
601 Receptors in Parkinson Disease: Novel Putative Chemoreceptors in the Human Brain. *Journal*
602 *of Neuropathology & Experimental Neurology* 72:524-539.
- 603 Heyne A, Kiesselbach C, Sahún I, McDonald J, Gaiffi M, Dierssen M, Wolffgramm J (2009) RESEARCH
604 FOCUS ON COMPULSIVE BEHAVIOUR IN ANIMALS: An animal model of compulsive food-
605 taking behaviour. *Addiction Biology* 14:373-383.
- 606 Kenny PJ (2011) Reward Mechanisms in Obesity: New Insights and Future Directions. *Neuron* 69:664-
607 679.
- 608 Lee NM, Carter A, Owen N, Hall WD (2012) The neurobiology of overeating. *EMBO reports* 13:785-
609 790.
- 610 Muretta JM, Mastick CC (2009) How insulin regulates glucose transport in adipocytes. *Vitamins and*
611 *hormones* 80:245-286.
- 612 Nora EP, Lajoie BR, Schulz EG, Giorgetti L, Okamoto I, Servant N (2012) Spatial partitioning of the
613 regulatory landscape of the X-inactivation centre. *Nature* 485.

- 614 Phipson B, Lee S, Majewski IJ, Alexander WS, Smyth GK (2016) ROBUST HYPERPARAMETER
615 ESTIMATION PROTECTS AGAINST HYPERVARIABLE GENES AND IMPROVES POWER TO
616 DETECT DIFFERENTIAL EXPRESSION. *The annals of applied statistics* 10:946-963.
- 617 Ramírez F, Bhardwaj V, Arrigoni L, Lam KC, Grüning BA, Villaveces J, Habermann B, Akhtar A, Manke
618 T (2018) High-resolution TADs reveal DNA sequences underlying genome organization in
619 flies. *Nature Communications* 9:189.
- 620 Rennie S, Dalby M, van Duin L, Andersson R (2018) Transcriptional decomposition reveals active
621 chromatin architectures and cell specific regulatory interactions. *Nature Communications*
622 9:487.
- 623 Ritchie ME, Phipson B, Wu D, Hu Y, Law CW, Shi W, Smyth GK (2015) limma powers differential
624 expression analyses for RNA-sequencing and microarray studies. *Nucleic acids research*
625 43:e47-e47.
- 626 Saper CB, Chou TC, Elmquist JK (2002) The need to feed: homeostatic and hedonic control of eating.
627 *Neuron* 36:199-211.
- 628 Sartorius T, Drescher A, Panse M, Lastovicka P, Peter A, Weigert C, Kostenis E, Ullrich S, Häring HU
629 (2015) Mice Lacking Free Fatty Acid Receptor 1 (GPR40/FFAR1) are Protected Against
630 Conjugated Linoleic Acid-Induced Fatty Liver but Develop Inflammation and Insulin
631 Resistance in the Brain. *Cellular Physiology and Biochemistry* 35:2272-2284.
- 632 Shi W, Oshlack A, Smyth GK (2010) Optimizing the noise versus bias trade-off for Illumina whole
633 genome expression BeadChips. *Nucleic acids research* 38:e204-e204.
- 634 Sisley S, Sandoval D (2011) Hypothalamic control of energy and glucose metabolism. *Reviews in*
635 *endocrine & metabolic disorders* 12:219-233.
- 636 Sweeney P, Yang Y (2017) Neural Circuit Mechanisms Underlying Emotional Regulation of
637 Homeostatic Feeding. *Trends in endocrinology and metabolism: TEM* 28:437-448.
- 638 Tanay A, Cavalli G (2013) Chromosomal domains: epigenetic contexts and functional implications of
639 genomic compartmentalization. *Current opinion in genetics & development* 23:197-203.
- 640 Volkow ND, Wang GJ, Tomasi D, Baler RD (2013) Obesity and addiction: neurobiological overlaps.
641 *Obesity reviews : an official journal of the International Association for the Study of Obesity*
642 14:2-18.
- 643 Warnes G, Bolker B, Lumley T gplots: Various R programming tools for plotting data. R package
644 version 2.6.0.
- 645 Yu G, Wang L-G, Han Y, He Q-Y (2012) clusterProfiler: an R Package for Comparing Biological Themes
646 Among Gene Clusters. *OMICS : a Journal of Integrative Biology* 16:284-287.
- 647 Zaborowski R, Wilczynski B (2016) DiffTAD: Detecting Differential contact frequency in Topologically
648 Associating Domains Hi-C experiments between conditions. *bioRxiv*.

649

650
651

Figures and figure legends

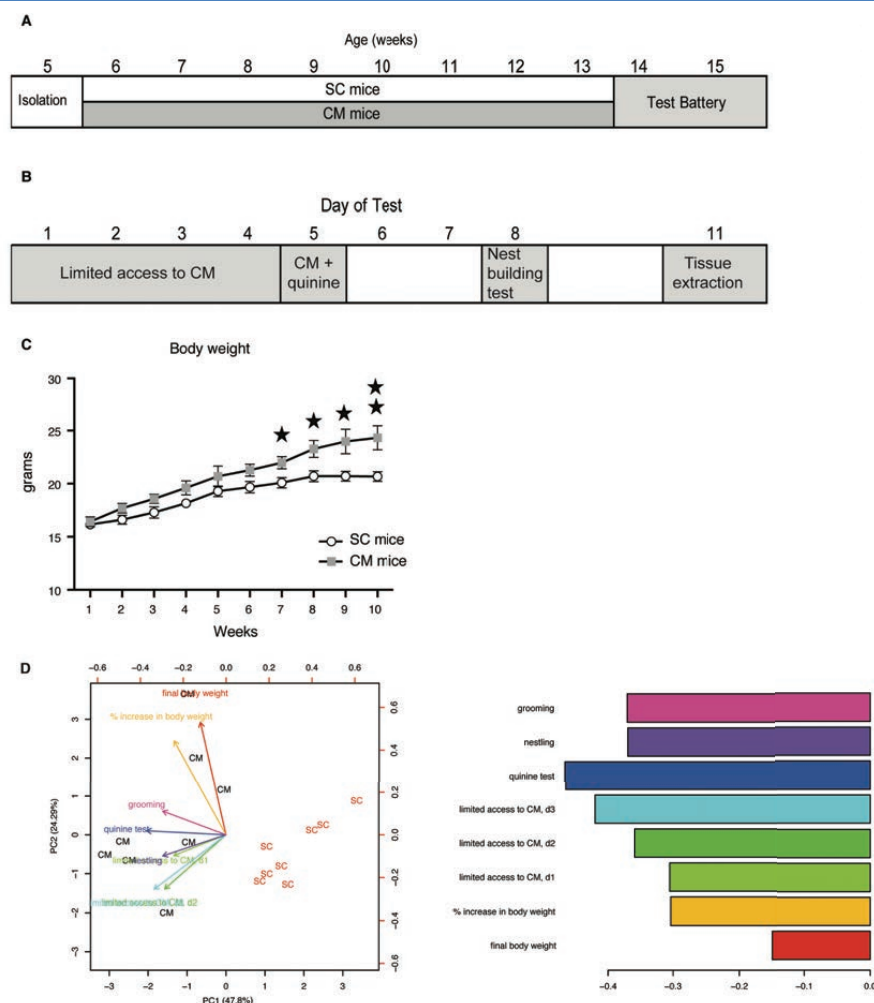


Fig 1. Free-access to a chocolate mixture leads to body weight gain

(A) Experimental schedule showing the age of mice along the experiment. Note that during the test battery animals continued receiving the same diet as during the weight gain phase (6 to 15 weeks of age). (B) Detail of the standardized testing battery used and the days of administration of each test. (C) Body weight (in g) changes with time in SC (white circles) and CM (grey squares) mice along the 10 weeks of the experiment. (D) Biplot of principal component analysis on SC and CM mice using bodyweight and eating-related behavioral variables indicated by colored arrows (left panel). Barplot showing the contribution of the variables to principal component 1 (right panel). Obesity was defined by the variables final body weight and percentage of body weight gain; compulsivity was evaluated by the CM intake during the 3 days of limited CM access, nest building behavior and grooming; inflexibility was explained by the amount of CM consumed in the quinine test.

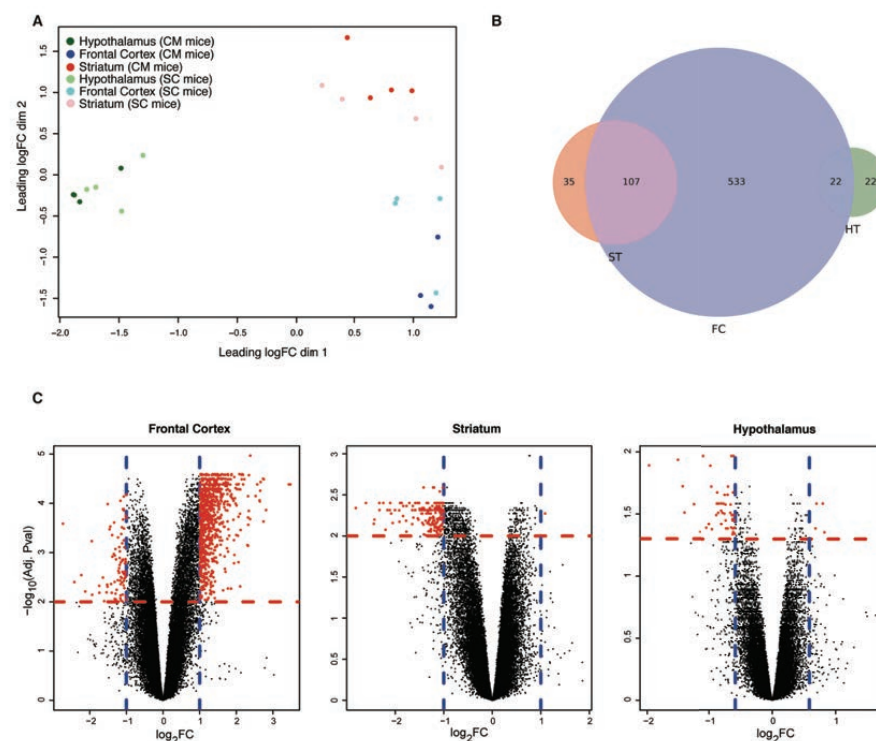


Fig 2. Differential expression analysis reveals that different brain areas present different transcriptional profiles when comparing SC and CM mice

(A) Multidimensional scaling plot with the top 500 most variable inter-group probes. HT, indicates the hypothalamic region (green dots); ST, the striatum region (red dots); FC the frontal cortex (blue dots); SC mice are represented with light colours; CM mice are coloured in dark colours. (B) Venn diagram showing the overlap among DE genes used for the enrichment analysis in the three brain areas (absolute fold-change ≥ 1.5 , adjusted p-value < 0.05 for hypothalamus, absolute fold-change ≥ 2 and adjusted p-value < 0.01 for the frontal cortex and the striatum). Colours represent the same brain areas as in A. Circles' areas are proportional to the gene counts. (C). Volcano plots for the three brain areas, on the x-axis \log_2 (fold changes), on the y-axis the significance ($-\log_{10}$ of the adjusted-p-value). Blue lines mark fold changes thresholds, red lines significance threshold. Each dot corresponds to a probe. Significant probes are marked in red.

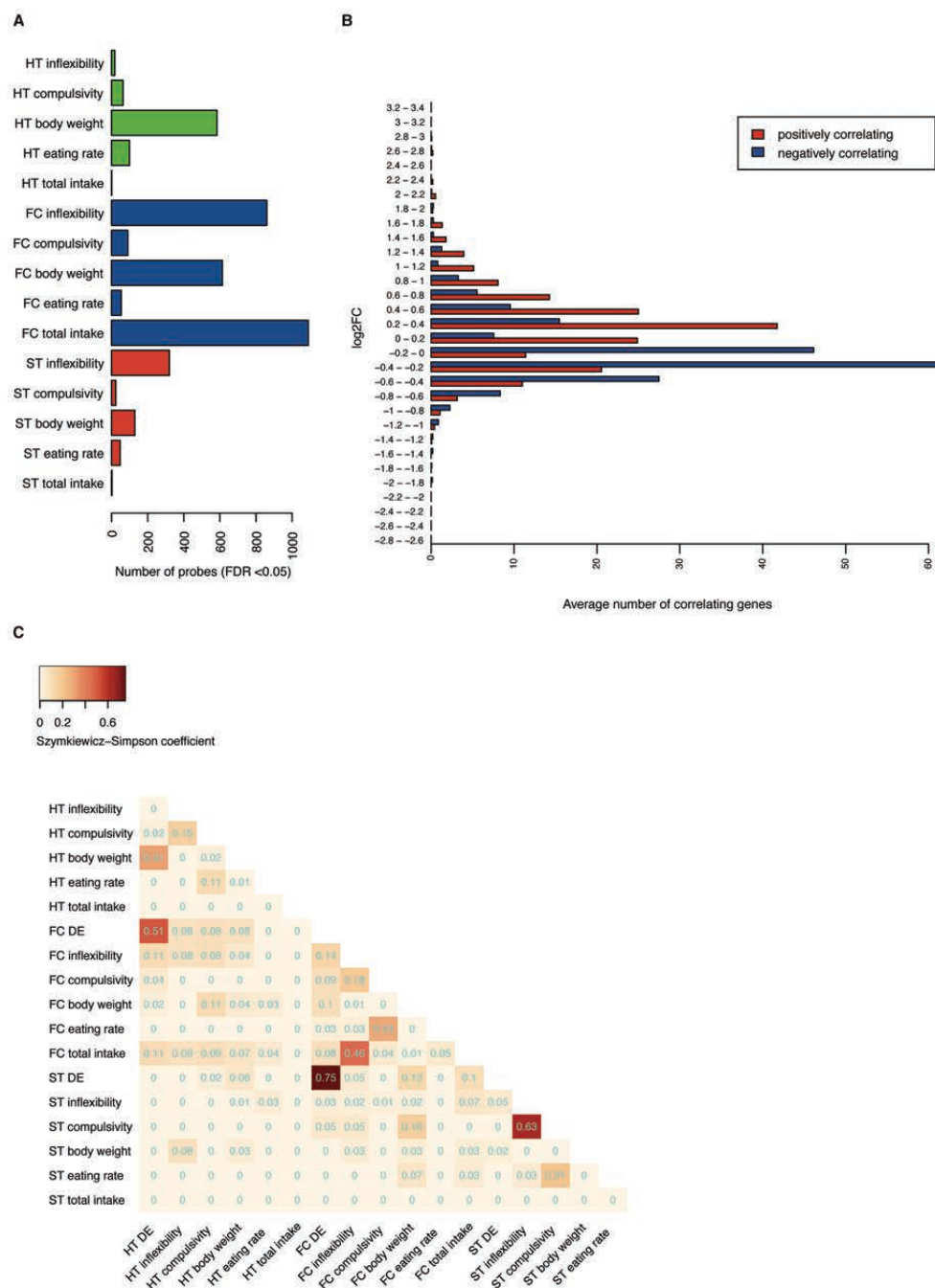


Fig 3. A subset of moderately expressed genes highly correlates with phenotypical changes

(A) Bar plot showing the number of genes correlating for each of the phenotypic variables that were detected with a false discovery rate < 5%. (B) Bar plot showing the average number of genes with an absolute rho higher than 0.9 for a given bin of log2 fold change (log2FC). The averages were calculated across all brain areas and variables. The majority of correlating genes have log2FC within 0.2 - 0.4 ranges (positive correlation marked in red and negative in blue). (C) Heatmap showing the Szymkiewicz-Simpson overlap coefficient between differentially expressed genes and genes correlating with eating-related variables. DE: differentially expressed genes. Brain region acronyms are the same as in Fig 2. Colour code according to the coefficient. Extended information related to the correlation between transcriptional changes with the physical/behavioural alterations could be found in Fig 3-1; Fig 3-2; Fig 3-3; Fig 3-4; Fig 3-5; Fig 3-6 and Fig 3-7.

690

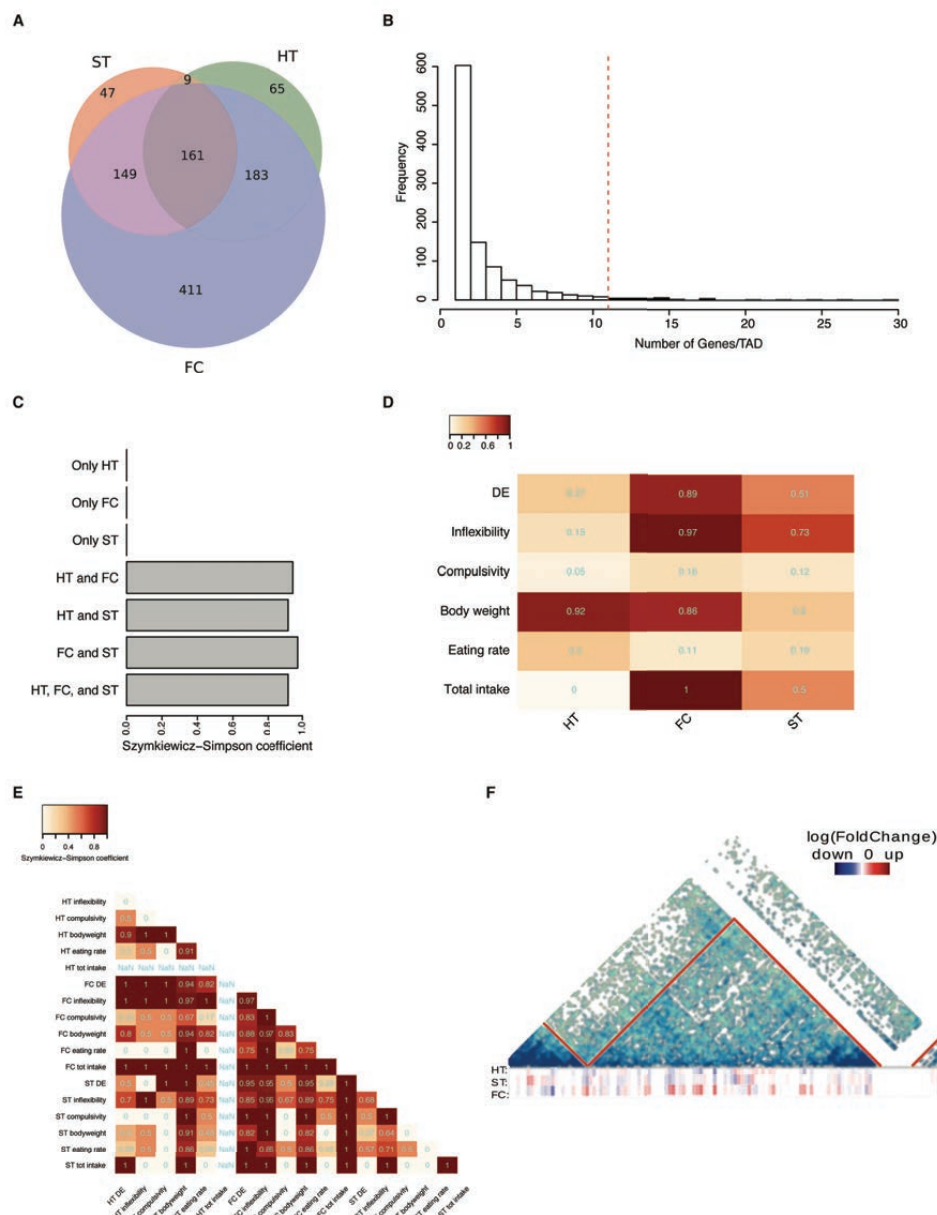


Fig 4. Co-regulation of genes within TADs (A) Venn diagram showing the overlap among TADs containing at least one DE or correlating gene in the three brain areas. Colours represent the same brain areas as in Fig 2A. Circles' areas are proportional to the gene counts. DE: differentially expressed genes. (B) Histogram showing the number of regulated genes per regulated TADs. The dashed red line demarks the 5% area of the distribution with TADs containing high number of regulated genes. Bars corresponding to these *regulated* TADs are on the right of the dashed line. (C) Bar plot showing the Szymkiewicz-Simpson overlap coefficient between *regulated* TADs with region specific or co-regulated TADs. Brain region acronyms are the same as in Fig 2. (D) Heatmap showing the Szymkiewicz-Simpson overlap coefficient between *regulated* TADs and TADs containing any of the DE or genes correlating with phenotypic variables (rows) in the three examined regions (columns). Brain region acronyms are the same as in Fig 2. Colour code according to the coefficient (E) For each group of DE or correlating genes we considered the subset of the 37 TADs on which the respective genes were mapping. The heatmap shows the overlap among those *regulated* TADs for each DE gene list, phenotypic variable, and brain region. The color-coded is proportional to the Szymkiewicz-Simpson overlap coefficient, which is also printed in cyan on the cells. (F) Hi-C map of TAD 624—example of a *regulated* TAD. TAD 624 is located on the chromosome 7: 109600000 - 113000000 bp. Three heatmaps at the bottom of the TAD represent expression of the genes localised within this TAD. Red colour depicts up- and blue colour down-regulation of the particular gene. Extended information related to the differential gene expression and correlating genes conformed within the TADs structure could be found in Fig 4-1 and Fig 4-2.

691
692
693
694
695
696
697
698
699
700
701
702
703
704
705
706

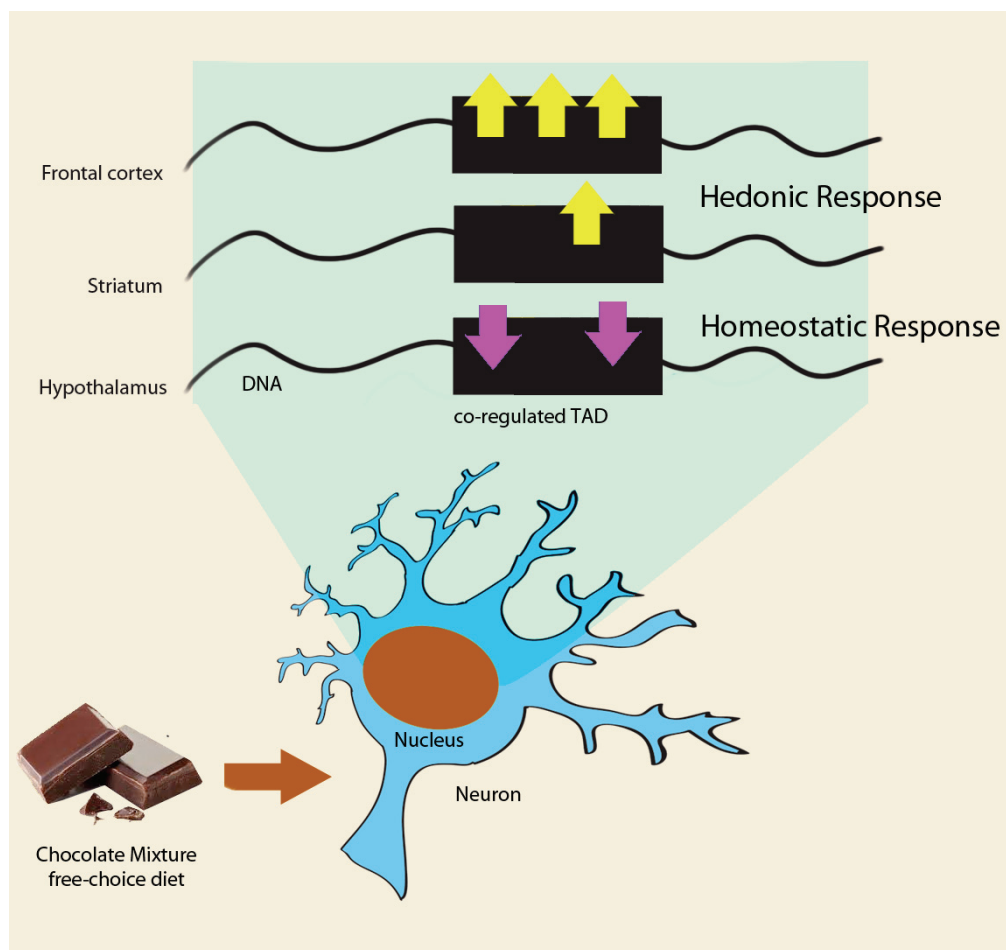
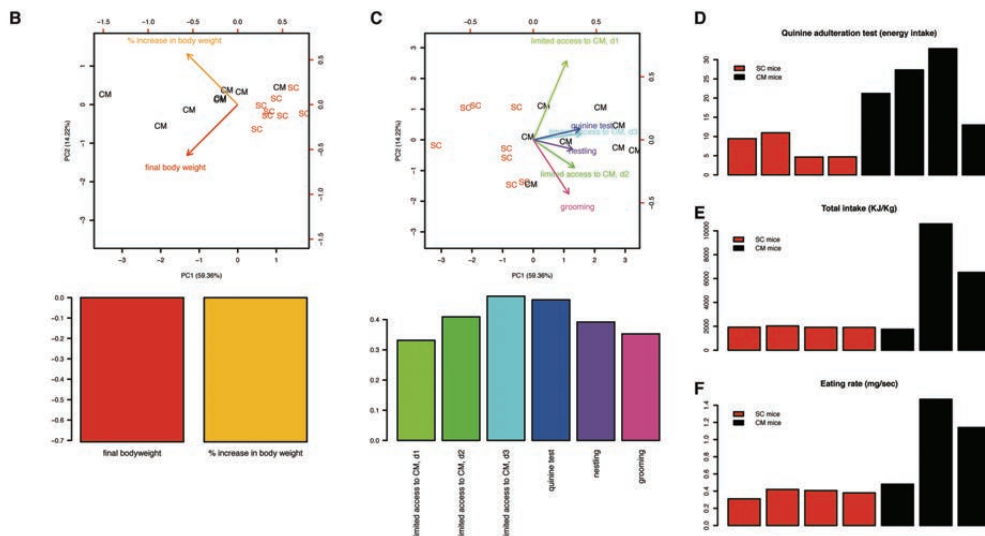


Fig 5. TADs orchestrate the transcriptional response both within and across brain areas. Cartoon depicting the response at the TADs level upon free choice chocolate mixture (CM) diet, in the nucleus of frontal cortex, striatum, or hypothalamus neurons. Differentially co-regulated TADs is simplified as a black box, with yellow arrows standing for upregulated genes, and purple ones downregulated genes.

714

715 Extended data



716

717

718 Fig 3-1. Correlation of transcriptional with behavioral analysis

719

720 (A) Biplot of principal component analysis on SC and CM mice using body weight variables indicated

721 by colored arrows (top) showing the clear separation between CM and SC mice. Barplot showing the

722 contribution of the body weight variables to the principal component 1 (bottom). (B) Biplot of principal

723 component analysis on SC and CM mice using behavioral variables indicated by colored arrows (top).

724 Barplot showing the contribution of behavioral variables to the principal component 1 (bottom). C-E

725 show the individual values of the variables used for gene expression correlation in SC mice (red) and

726 CM mice (black). Note that eating rate and total intake values were only available for three of the four

727 individuals used for the transcriptome analysis. (C) Barplot showing the differences in CM energy

728 intake of SC and CM mice in the quinine adulteration test. (D) Barplot showing the differences in total

729 energy intake of standard chow and chocolate mixture (CM mice). Data from one of the mice in the

730 CM group were missing. (E) Barplot showing the differences in eating rate of standard chow (SC

731 mice) and chocolate mixture (CM mice).

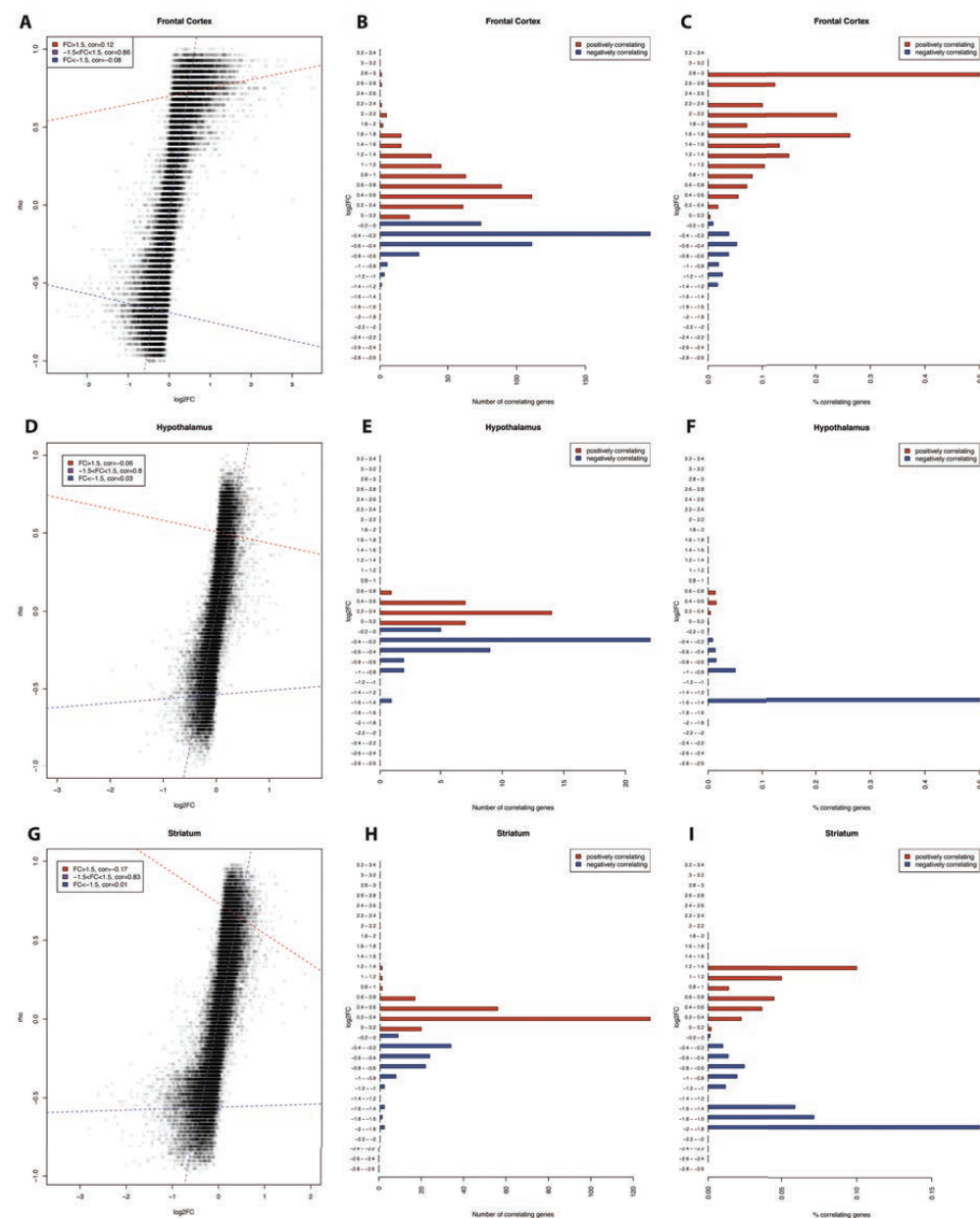


Fig 3-2. Genes correlating with inflexibility

(A) Dot plot showing the rho score for inflexibility (x-axis) and the log2FC (y-axis) in frontal cortex. Each dot is a microarray probe. (B) Barplot showing how many genes with an absolute rho higher than 0.9 for a given bin of log2 Fold change. (C) Same as in B normalized for the total number of genes present in a given bin of log2 Fold change. (D, E, F) Same as in A, B and C for striatum. (G, H, I) Same as in A, B and C for hypothalamus

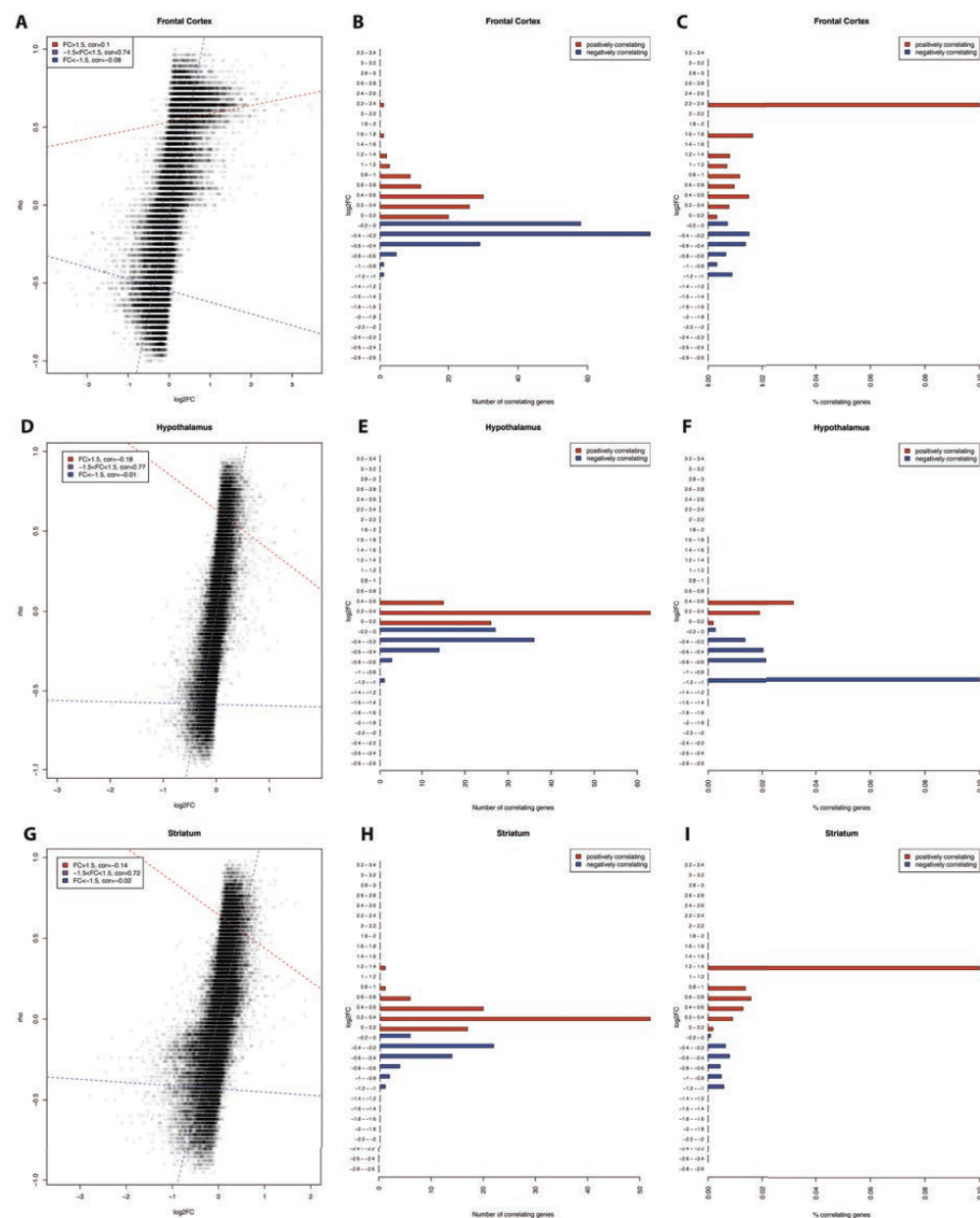


Fig3-3 . Genes correlating with compulsivity

(A) Dot plot showing the rho score for compulsivity (x-axis) and the log2FC (y-axis) in frontal cortex. Each dot is a microarray probe. (B) Barplot showing how many genes with an absolute rho higher than 0.9 for a given bin of log2 Fold change. (C) Same as in B normalized for the total number of genes present in a given bin of log2 Fold change. (D, E, F) Same as in A, B and C for striatum. (G, H, I) Same as in A, B and C for hypothalamus

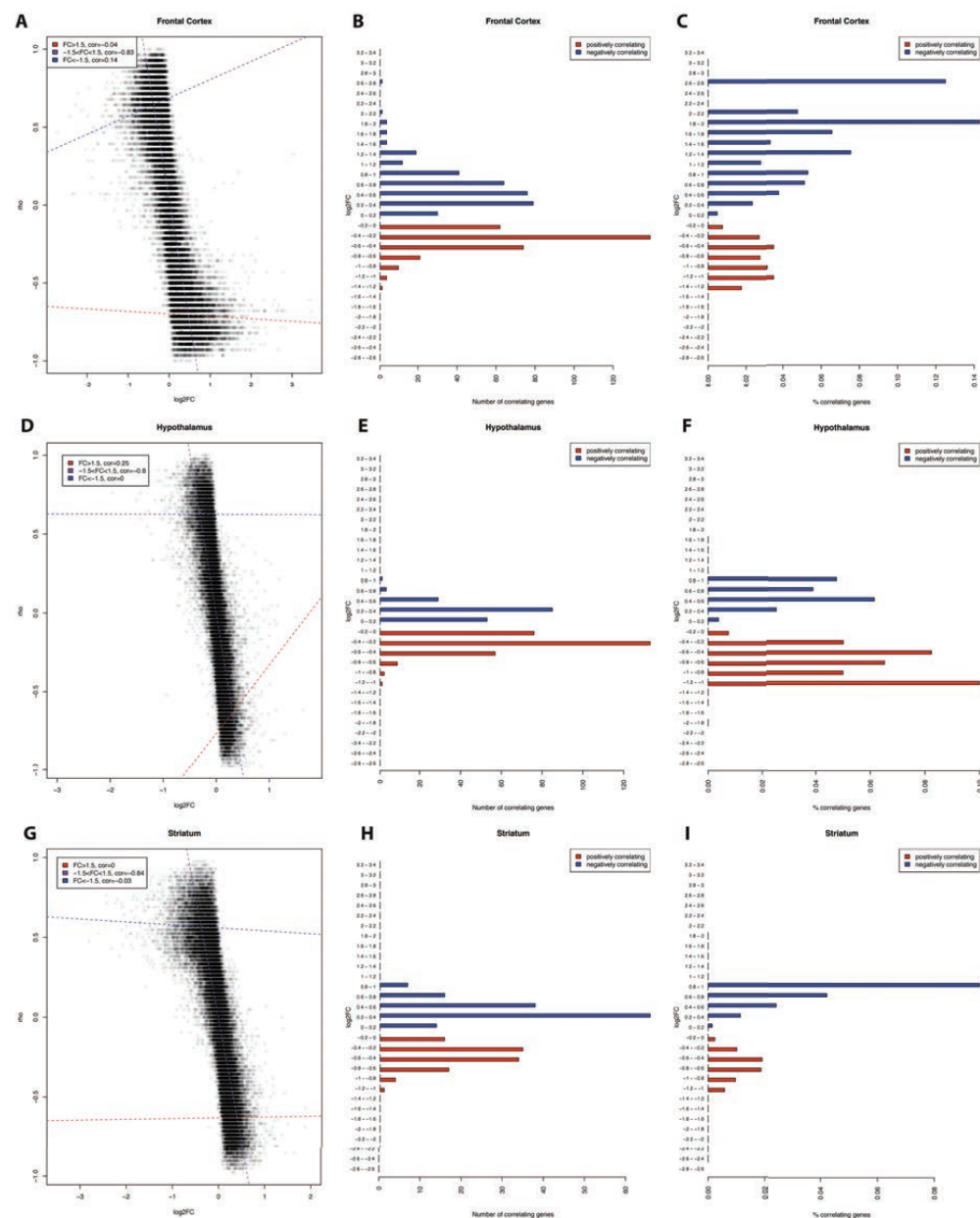


Fig 3-4. Genes correlating with body weight

(A) Dot plot showing the rho score for body weight (x-axis) and the log2FC (y-axis) in frontal cortex. Each dot is a microarray probe. (B) Barplot showing how many genes with an absolute rho higher than 0.9 for a given bin of log2 Fold change. (C) Same as in B normalized for the total number of genes present in a given bin of log2 Fold change. (D, E, F) Same as in A, B and C for striatum. (G, H, I) Same as in A, B and C for hypothalamus

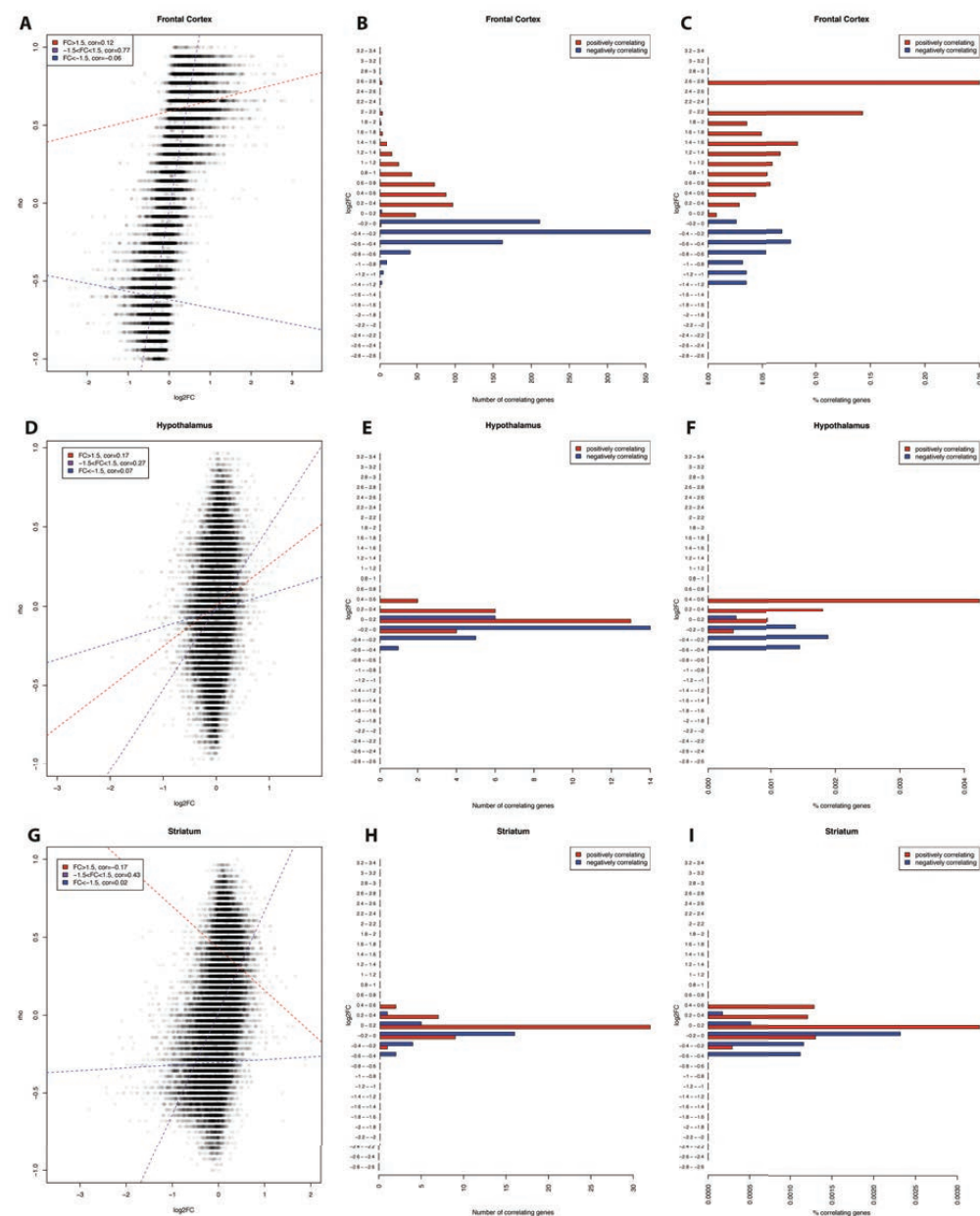


Fig 3-5. Genes correlating with eating rate
 (A) Dot plot showing the rho score for eating rate (x-axis) and the log2FC (y-axis) in frontal cortex. Each dot is a microarray probe. (B) Barplot showing how many genes with an absolute rho higher than 0.9 for a given bin of log2 Fold change. (C) Same as in B normalized for the total number of genes present in a given bin of log2 Fold change. (D, E, F) Same in A, B and C for striatum. (G, H, I) The same in A, B and C for hypothalamus

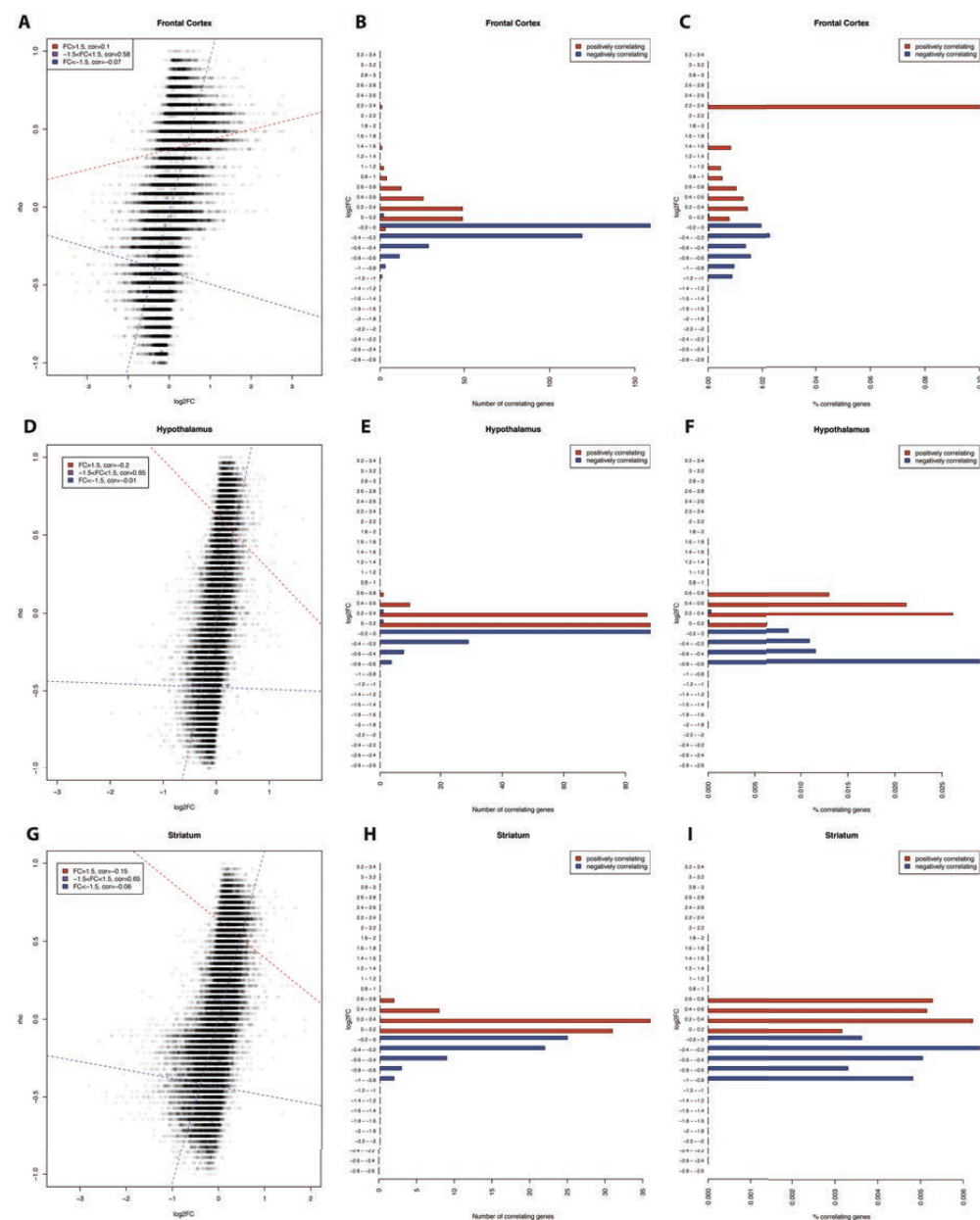


Fig 3-6. Genes correlating with total intake

(A) Dot plot showing the rho score for total intake (x-axis) and the log2FC (y-axis) in frontal cortex. Each dot is a microarray probe. (B) Barplot showing how many genes with an absolute rho higher than 0.9 for a given bin of log2 Fold change. (C) Same as in B normalized for the total number of genes present in a given bin of log2 Fold change. (D, E, F) Same as in A, B and C for striatum. (G, H, I) Same as in A, B and C for hypothalamus

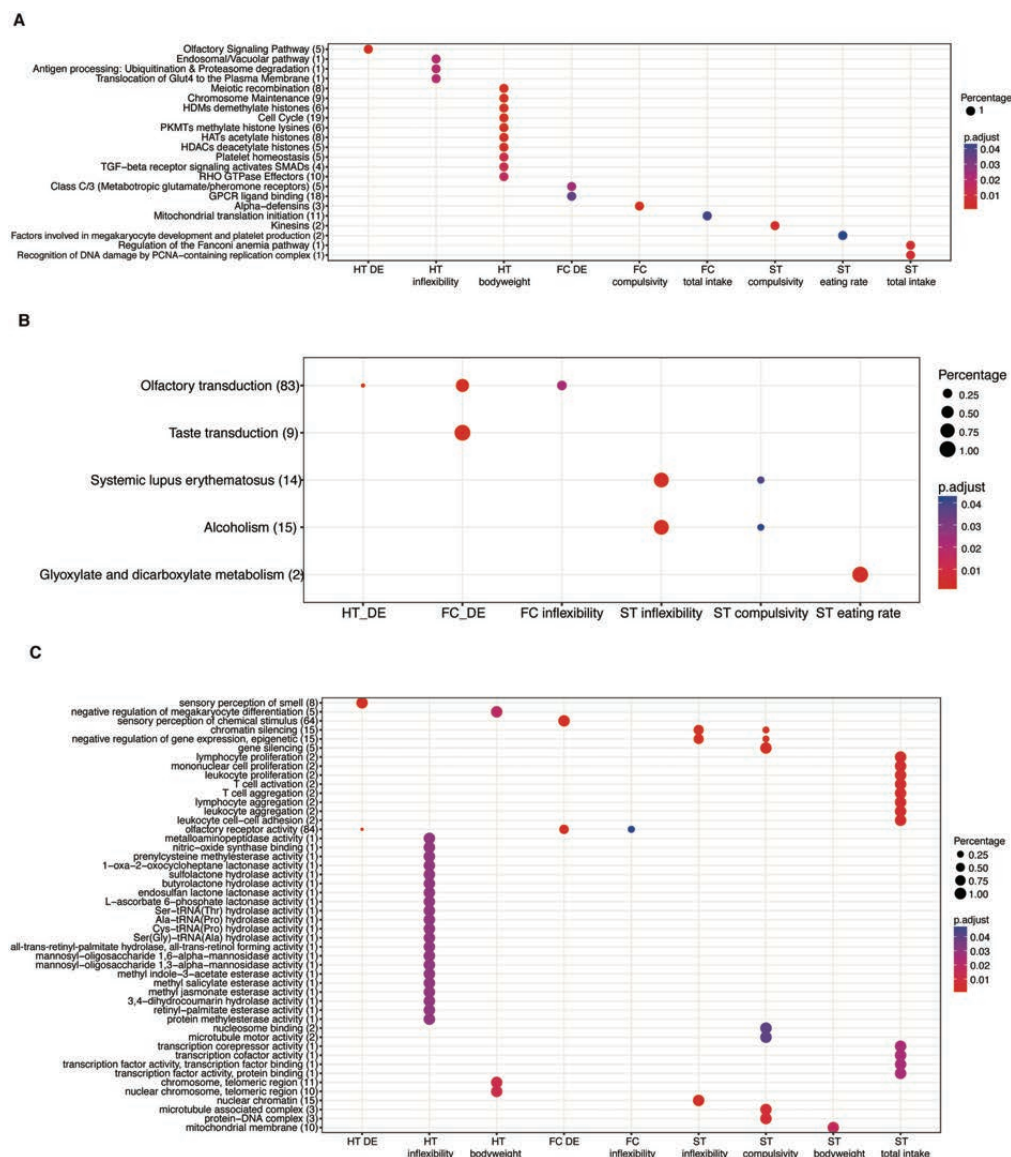


Fig 3-7. DE and correlating genes are enriched in region specific molecular pathways (A) REACTOME enrichment analysis for DE and correlating genes in the three brain areas. The color-gradient indicates the adjusted p-value for the enrichment. Number in parentheses indicates the number of identified genes in each category. Dot size corresponds to (gene count for each group)/(total gene count for each category). In case of overlapping categories, only the most significant one is shown (see *Methods*). (B) KEGG enrichment analysis for DE and correlating genes in the three brain areas. The color-gradient indicates the adjusted p-value for the enrichment. Numbers in parentheses indicate the number of identified genes in each category. Dot size corresponds to (gene count for each group)/(total gene count for each category). In case of overlapping categories, only the most significant one is shown (see *Methods*). (C) GO enrichment analysis for DE and correlating genes in the three brain areas. The color-gradient indicates the adjusted p-value for the enrichment. Numbers in parentheses indicate the number of identified genes in each category. Dot size corresponds to (gene count for each group)/(total gene count for each category). In case of overlapping categories, only the most significant one is shown (see *Methods*). Only pathways with an FDR < 5% are shown.

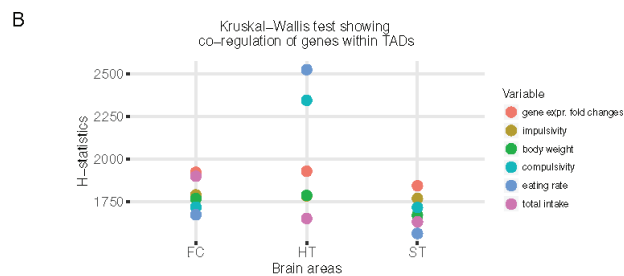
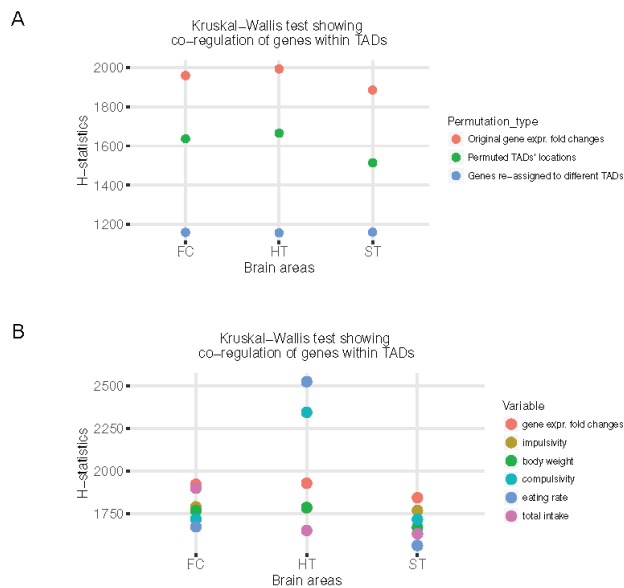


Fig. 4-1. DE and correlating genes conformed within the TADs structure
A) Kruskal-Wallis tests H-statistics illustrating distribution of variance of gene expression fold changes among TADs (red dots) and the permuted gene expressions in the frontal cortex (FC), hypothalamus (HT) and striatum (ST). B) Kruskal-Wallis tests H-statistics illustrating distribution of variance of gene expression fold changes among TADs (red dots) and correlations of gene expressions with phenotypical variables (other colors) in the frontal cortex (FC), hypothalamus (HT) and striatum (ST).

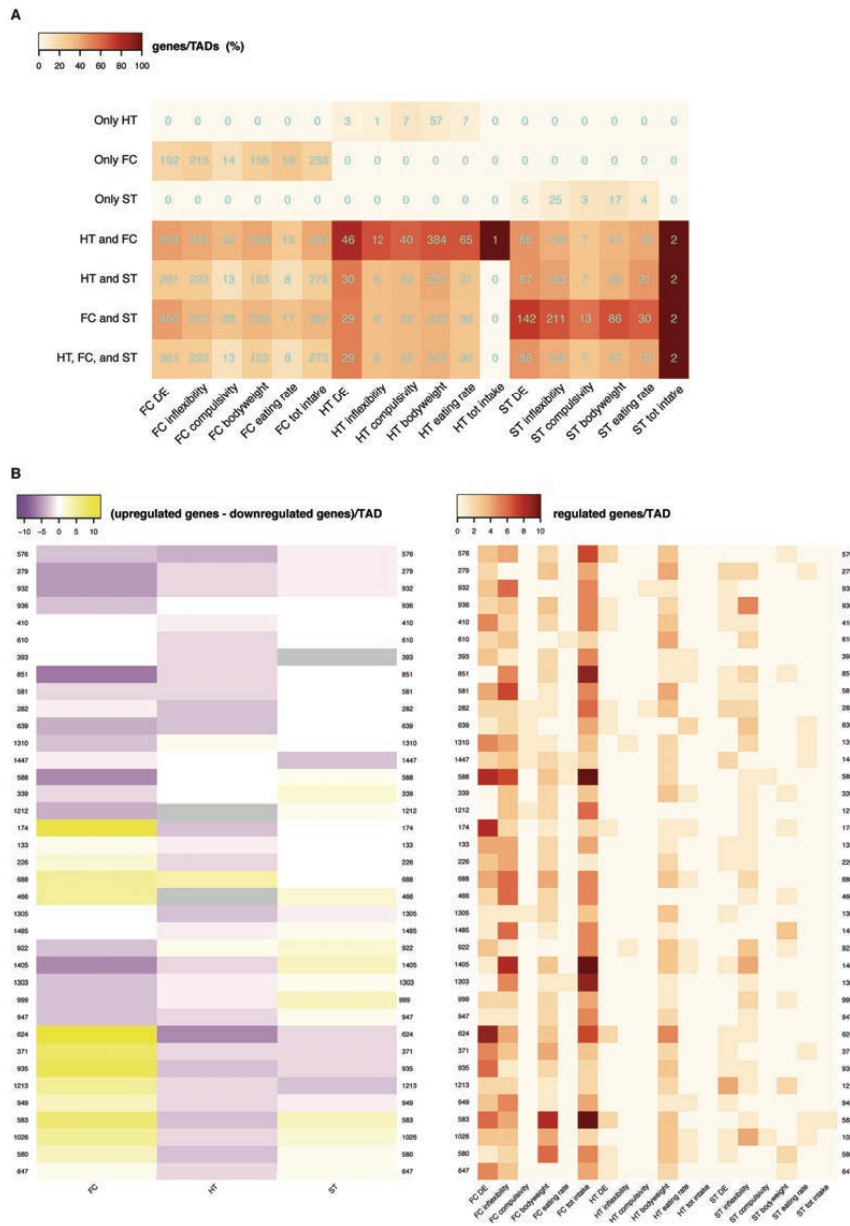


Fig 4-2. (A). Heatmap showing the percentages of counts of the genes contained in the TADs set from Fig 4A over the DE gene and phenotypical variables for each brain area. Actual gene numbers are printed in cyan. (B) *Left side*. Heatmap where each row corresponds to a *regulated* TAD, each column to a brain region. The color code indicates the difference between upregulated and downregulated genes number (considering only DE and correlating genes), from yellow (more up-regulated genes), to violet (more downregulated genes), passing for white (equal number). Gray boxes are TADs without any regulated genes for that specific region. *Right side*. Heatmap where each column corresponds to DE and correlating genes for each brain region, and each row to a *regulated* TADs. The color code indicates the actual number of genes per each TADs in a given category.

808 EXTENDED DATA

809

810 Extended data 1. Zip file containing the R mark Down file with the code to reproduce all the
811 analyses performed in R.

812

813 Extended data 1-1. Table with the behavioral and physical data collected.

814

815 Extended data 2-1. Differential expression analysis for the frontal cortex.

816

817 Extended data 2-2. Differential expression analysis for the striatum.

818

819 Extended data 2-3. Differential expression analysis for the hypothalamus.

820

821 Extended data 3-1. Results for the REACTOME enrichment analysis.

822

823 Extended data 3-2. Results for the KEGG enrichment analysis.

824

825 Extended data 3-3. Results for the Gene Ontology enrichment analysis.

826

827 Extended data 4-1. Mapping between the probes of the microarray and the TAD analyzed in
828 our study. Only uniquely mapping probes were considered.

